# CHALMERS

# ABB

# On Moving Contacts in On-Load Tap Changers

Johan Hillergren and Martin Lindahl

Master of Science Thesis (30 hp) in the
Master Degree Programme Applied Physics

Performed at ABB Components AB in Ludvika, Sweden

## On Moving Contacts in On-Load Tap Changers

Authors: Johan Hillergren and Martin Lindahl
Contact: johan.hillergren@gmail.com, m.lindahl@gmail.com

Applied Physics
Chalmers University of Technology
SE-412 96 Gothenburg
Sweden
Tel: +46 (0)31 - 772 10 00

ABB Components
SE-771 80 Ludvika
Sweden
Tel: +46 (0)21 - 32 50 00

**Abstract**

This is a Master's thesis in Applied Physics. The primary topic of the thesis is to develop an accelerated life test for the moving contacts in on-load tap changers, simulating the wear of 30 years use regarding oxidation and coking. The secondary topic is to examine the surface structure of silver contacts to aid in understanding how silver iodide contacts can have the superb electrical properties of silver contacts, but with much better frictional properties.

The accelerated life test simulates the wear on the contacts of the OLTC, stemming from oxidation, coking and thermal deformations, during the course of 30 years in only 30 days. The thesis begins with a theoretical background on electrical contacts, tap changers and accelerated testing. It then treats the theoretical derivation of the test parameters. An evaluation test is set up and performed to evaluate the feasability and merit of the test. The results are promising, as the contacts performed as expected with the contact pairs copper/brass performing poorly, copper/silver performing acceptedly and silver/silver performing exceptionally.

The surface structure examination begins with a wear process, where sliding silver and silver iodide contacts are worn using an on-load tap changer operating 400 times to create a worn track on the contacts. The contact surfaces are then observed in a scanning electron microscope in search for pores and crevices where iodide could accumulate. These pores and crevices are found, although the accumulation of silver iodide in these not can be proven at this point. That the pores now are shown to exist on the surfaces is a step in the right direction regarding the accumulation hypothesis. It is a necessary but not sufficient criterion for the accumulation hypothesis to be true.

I

# Contents

IV

# Preface

This Master's thesis is the final project for recieveing the Master of Science degree in Applied Physics at Chalmers University of Technology. The background work to the thesis was carried out at ABB Components AB in Ludvika between February and June 2010. The aim is that a person with an applied physics background should be able to follow the report without consulting other material, and an expert in the field of tap changers should find the results interesting.

We would like to thank our managers, Gerd Chalikia and Henrik Sundberg for supporting our ideas even when costs were piling, Gunnar Andersson, Martin Wåhlander, Mattias Lindquist and Tommy Larsson for providing their expertise and experience, everybody else at the TU department, Lars, Hans and Calle at the laboratory for helping us set up and run the evaluation test, and our examinor at Chalmers, Göran Wahnström.

Above all though, we would like to thank Christer Arnborg for lending us his expertise, enthusiasm, help, time, network and support in all daily work, from the very first day to the last.

Johan and Martin

# Nomenclature

| | |
|---|---|
| $[O_2]$ | Oxygen concentration in ppm by volume |
| $\Delta l$ | Thermal deformation length in meters |
| $\Delta T_b$ | Amplitude of bulk temperature change in kelvins |
| $\Delta T_o$ | Amplitude of oil temperature cycle in kelvins |
| $\tau$ | Time interval |
| $\tau_i$ | Duration of time interval $i$ |
| $\tau_I$ | Time at maximum load current per cycle |
| $\tau_o$ | Time at maximum oil temperature per cycle |
| $a$ | Arrhenius acceleration factor or general constant |
| $A$ | Rate constant |
| AAFL | Accelerated aging functional life test |
| Ag | Silver or silver contact |
| Ag/Ag | Fixed electroplated silver contact with sliding wrought silver contact |
| Ag(p) | Electroplated silver contact |
| Ag(p)/Ag(p) | Fixed electroplated silver contact with sliding electroplated silver contact |
| Ag(p)/Ag(s) | Fixed electroplated silver contact with sliding wrought silver contact |
| Ag(s) | Wrought silver contact |
| AgI | Silver |
| AgI(p) | Electroplated silver contact coated in silver iodide |
| AgI(p)/Ag(p) | Fixed electroplated silver contact coated in silver iodide with sliding electroplated silver contact |
| AgI(p)/Ag(s) | Fixed electroplated silver contact coated in silver iodide with sliding wrought silver contact |
| AgI(p)/AgI(s) | Fixed electroplated silver contact coated in silver iodide with sliding wrought silver contact coated in silver iodide |
| AgI(s) | Wrought silver contact coated in silver iodide |
| Brass | Brass contact |
| Cu | Copper or copper contact |
| Cu/Brass | Fixed copper contact with sliding brass contact |
| Cu/Ag | Fixed copper contact with sliding wrought silver contact |

| | |
|---|---|
| $E$ | Activation energy |
| EDX | Energy-dispersive x-ray spectroscopy |
| EHT | Electron high tension |
| $k$ | Boltzmann's constant |
| $I$ | Current in ampere |
| $I_r$ | Rated current for on-load tap changer |
| $l_o$ | Original length before thermal deformation in meters |
| $N_I$ | Number of current cycles per day |
| $N_o$ | Number of oil cycles per day |
| O | Oxygen |
| OLTC | On-load tap changer |
| $P$ | Power in watts |
| S | Sulfur |
| SEM | Scanning electron microscope |
| $t$ | Time in seconds |
| $T$ | Temperature in kelvins |
| $T_b$ | Bulk temperature in kelvins |
| $\Delta T_{b/o}$ | Bulk temperature rise over oil temperature in kelvins |
| $T_c$ | Contact spot temperature in kelvins |
| $T_o$ | Oil temperature in kelvins |
| $\Delta T_{tr/a}$ | Maximum allowed bulk temperature rise over ambient |
| $\Delta T_{s/b}$ | Super temperature, the rise of the contact spot over the bulk temperature in kelvins |
| $U$ | Voltage in volts |

# List of Figures

# List of Tables

# 1   Introduction

The large scale transformers operating on national level electricity grids need to be regulated when operating conditions change. When, for example, people wake up in the morning and start to consume more electric power the potential in the grid tends to decrease. By mechanically regulating the turn ratio in the transformer, the on-load tap changer (OLTC) can keep the grid potential at a sufficiently constant level.

Since the OLTC is the only moving component of the transformer it is particularly vulnerable. Approximately half of all transformer failures are caused by failures in the OLTC. The reasons for these failures can be many and different failure modes are important under different operating conditions. Such failure modes contain mechanical wear of the contacts, excessive oxidation, coking, fretting and creep.

The purpose of the present thesis is to design a test method to test OLTC contacts regarding oxidation and coking endurance. Further, a study of contact surfaces using scanning electron microscopy (SEM) is to be performed to explain how silver iodide (AgI), as a solid lubricant, can still remain on OLTC contacts after thousands of operations.

The acceleration in the oxidation endurance test will be theoretically derived using the Arrhenius relation stating that the reaction speed of applicable chemical reactions doubles for each $10\,°C$ of increased temperature. The test method is delimited to test moving OLTC contacts operating in oil. With the achieved acceleration, each day of testing corresponds to one year of real life operation. The test method itself is then verified by performing a test with three different types of contacts which, from field experiences, are expected to perform differently in the test. The test method is found to be valid.

The study of contact surfaces is performed both on worn and unworn OLTC contacts which are used in production units. Large data quantities will not be gathered in this thesis, so that no broad conclusions can be drawn but the results are instead intended to provide possible explanations of the lasting low friction of AgI contacts. Pores and crevices are found on the contact surfaces, indicating that the AgI could accumulate in these even after a large number of operations.

In this thesis a theoretical background is first given in section 2. Here fundamental concepts of electrical contacts as well as accelerated aging and failure modes of the OLTC are described. The oxidation endurance test will then be thoroughly described in section 3, with a theoretical motivation of the test and the methodology of the performed verification test. In section 4, the methodology of the surface structure study is described. The results of both

the oxidation endurance test and the surface structure study are presented in section 5, followed by a discussion of the thesis' results in section 6.

# 2 Theory

The theory section provides basic knowledge for those who do not regulary work with contacts or on-load tap changers. It also contains a compilation of failure modes for on-load tap changers, which might be of interest for people in the business as well. It also has an introduction to accelerated testing, silver iodide as a contact material and to scanning electron microscopy.

## 2.1 On-Load Tap Changers

The on-load tap changer (OLTC) adds the possibility to regulate the output voltage of a power transformer by changing the turn ratio whilst the transformer is under load. The large currents and voltages under which the transformer operates impose great demands on the contacts of the OLTC. It is expected to stay in operation for at least 30 years with only minor maintenance, and since the functioning of the power grid is fundamental in today's society, the robustness of the OLTC also has to be substantial.

A typical case is that the OLTC can regulate the transformer voltage $\pm 20\%$ of its standard value. This is done discretely in 9 to 35 steps [1]. In normal grid situations the OLTC is operated around 10 times per day, but this number can be much higher in for example industrial applications. It might also not be operated at all for long periods of time, even years. Most OLTCs consist of two types of switching devices: the diverter switch and the tap selector. The diverter switch is used to control which way the current is taking in the OLTC, and is thus switching under load. The tap selector chooses which of the regulating windings that is to be used at present.

There are a number of steps performed in sequence to complete a switching operation. How this is done for an OLTC with a diverter switch and a selector is shown in figure 1. The contacts x and v, called the main contacts, are the two possible states for the diverter switch while V and H are the two selector arms which select the one of the numbered tap contacts to choose the number of turns that are presently used of the regulating winding. There are also two help contacts, y and u, with a resistor each [2]. With the denomination of figure 1, the sequence to change regulation winding from tap position 6 to tap position 5 is as follows:

(a) The initial state. The load current goes through x and V to tap 6. The selector arm H is currently off-load.

(b) Since selector arm H is off-load it can be operated from tap 7 to tap 5.
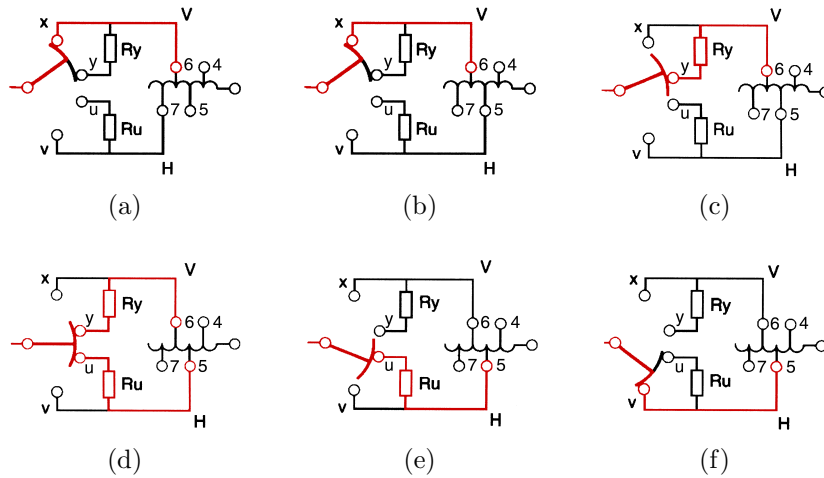
Figure 1: Switching sequence from tap position 6 to tap position 5 in an OLTC with a diverter switch and selector. See text body for a detailed description of the different steps. Figures from [2]. (In color)

**(c)** The diverter switch starts to move from main contact x towards main contact v. The load current now goes through help contact y and its resistor.

**(d)** In this transition state the load current is handed over from help contact y to help contact u. There is a circulation current present between these contacts, but its magnitude is limited by the resistors. Current is now passing through tap 5.

**(e)** The help contact y has opened and the load current now solely passes through help contact u and tap 5.

**(f)** The final state is reached. The load current now goes through v and H to tap 5. Selector arm V is off-load and is available to take another step to tap position 4 if this is needed.

As seen, the tap selector always operates off-load in contrast to the diverter switch.

## 2.2 Electrical Contacts

The electrical contacts are a critical issue in the OLTC. Since the power transmitted through the OLTC is great, it is necessary to keep the resistances as low as possible, since an increasing resistance also will cause increasing losses through heat dissipation. As will be treated later, increased heat at
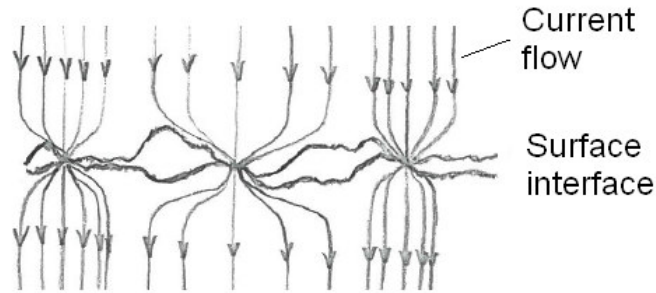
Figure 2: Schematic image of the interface between two contact surfaces. The points where the surfaces are in electrical contact and, the current flow between them take place, are called *a*-spots.[3, p. 2]

the contact point may also lead to resistance increasing further, creating a self-increasing process, a resistance runaway. Though not the only problem in OLTCs, it is a major one in the long time operability. Here, some basic contact theory will be treated for the unfamiliar reader.

First of all, it is important to know that the appearance of two contact surfaces might be deceptive. They might seem to cover a large area and seem smooth. On the microscale where the current is transferred, they are normaly very rough though. Only a small amount of the area is actually in electric contact, see figure 2. Asperities from both contact surfaces will come into contact and prevent the contacts to approach each other any further. These points where the contacts touch are known as *a*-spots. These *a*-spots impose a geometrical constriction to the electron transfer between the two surfaces giving rise to an increased resistance in the interface between two surfaces.[3, p. 1] Because of materials ability to deform to adapt to a meeting surface, increased pressure between two contacts will result in more asperities reaching each other. More *a*-spots will thus be created, allowing the current more passage ways and lowering the resistance, much in the same way as parallel resistors do. Decreased contact pressure will ofcourse have the opposite effect. This also makes contact resistance dependent of the hardness of the materials, since two hard materials will have less ability to deform.[3, p. 11]

Another important knowledge is how the contact temperatures vary with current. The bulk temperature of OLTC contacts are generally said to be proportional to the current raised to the 1.6th power [4, p. 35]. The equation

$$T \propto I^{1.6} \tag{1}$$

will be used on numerous occation in the thesis. In the *a*-spots, the temperature increases even further. From [3, p. 51] we know that the temperature

5

of an electrically heated $a$-spot can be calculated from

$$U^2 = 4L(T_c^2 - T_b^2) \tag{2}$$

where $L = 2.45 \cdot 10^{-8} \, \mathrm{V^2 K^{-2}}$ is the Lorenz constant [3, p. 50] and $T_c - T_b$ is the supertemperature (denoted $\Delta T_{c/b}$) which is the deviation of the $a$-spot temperature ($T_c$) from the bulk connector temperature ($T_b$).

## 2.3 Failure Modes of OLTC Contacts

To be able to design a relevant endurance test for OLTCs it is important to first analyze the different failure modes that can lead to an OLTC contact failure. These failures can stem from widely disparate phenomena such as chemical or mechanical wear. The identified failure modes are here explained and discussed one at a time. A concluding discussion is then held in section 3.5 about which failure modes to include in the proposed endurance test.

### 2.3.1 Oxidation

Oxidation is one part of a reduction-oxidation reaction, or more commonly, a redox reaction. A redox reaction is a chemical reaction where both reduction and oxidation take place. An oxidation is merely a loss of electrons, or an increase oxidation number, by an atom, ion or molecule to an other atom, ion or molecule, which is reduced, the other part of the redox reaction. The substance losing electrons is called a reducing medium and the substance that accepts the electron as an oxidizing medium. The reaction does not, as the name might imply, necessarily include oxygen, altough it is common. The most common materials in OLTC contacts are copper and silver. Two redox reactions with these materials, one including oxygen, the other not, are:

$$2\mathrm{Cu} + \mathrm{O} \rightarrow \mathrm{Cu_2O}$$

$$2\mathrm{Ag} + \mathrm{S} \rightarrow \mathrm{Ag_2S}$$
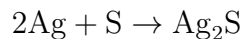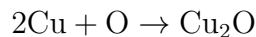
Oxidation give rise to insulating or weakly conducting surface films on contacts, increasing contact resistance [3, p. 36]. The oxidation layer will continue to grow as long as the contact material has access to the oxidizing agent. If diffusion through the oxidized layer is too hard, the process will stop [3, p. 93]. This phenomenon is commonly called passivation.

Increased resistance is a problem since it increases impedance and losses in the transformer. The allowed impedances and losses and the way they are

evaluated are different in different standards, e.g. IEEE standard C57.12.00 [5] allows a $\pm 10\%$ tolerance from the transformer loss specification. If the OLTC contacts are too heavily oxidized, they may contribute to to the losses reaching these levels.

### 2.3.2   Coking

When carbon is extracted from the surrounding oil and is deposited on a contact it is said that a coking process is taking place. The coking process is a chemical reaction where pyrolitic carbon is created [6]. In general this happens when the contact is very hot so that the activation energy is available to start the chemical reactions which the coking consists of.

The process is initiated by the formation of a thin oil film on the contact [6]. The oil film, which consists of polymerized oil, reduces the conduction of the contact spot, thus leading to higher resistance. The higher resistance will in turn generate more heat which induces the formation of a thicker oil film layer.

After this process has been going on for some time the temperature has reached high enough values for the coking itself to start. This is when the temperature is close to $200\,°C$ above the surrounding's temperature [7]. The layer of carbon which is formed on the contact surface will now influence the contact in two ways. First, it will further reduce the conduction of the contact spot, leading to even higher contact resistance and more heat generation. Second, it will lower the thermal conduction away from the contact spot and will thus act as a heat insulator. The insulation properties originate from the fact that the coke layer is microporous which lowers the oil flow [6, 7]. This in turn will raise the contact temperature further. As this is a self-increasing process, eventually thermal runaway will occur leading to complete contact failure [6].

### 2.3.3   Mechanical Wear

Mechanical wear is defined as "the loss of particulate material from solid surfaces as a result of mechanical action" [3, p. 310]. There are two fundamental types of mechanical wear relevant for OLTC contacts; abrasive and adhesive wear. In the first type, abrasive wear, a protrusion of one contact cuts into another contact forming a groove. The contact surfaces become very rough when abrasive wear takes place and this makes it more probable that adhesive wear (explained below) will take place, or even interlocking of the two contacts [8, p. 232].

In the second type, adhesive wear, the two contact surfaces cold weld and
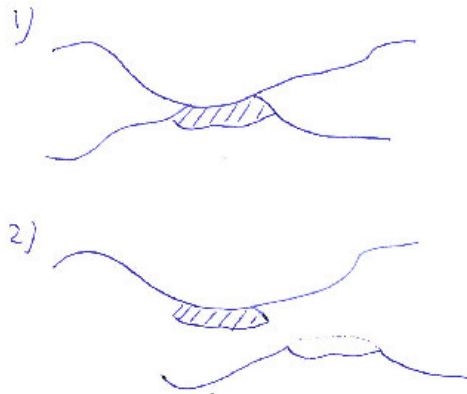
Figure 3: Schematic illustration of adhesive wear. The striped area is initially part of the lower surface (1), but adheres to the top surface and is ripped loose (2) when relative movement occurs. Based on [8].

a subsequent movement break the attachment at a position different from the original cold weld. This is schematically depicted in figure 3. If the strength of the cold is greater than the strength of the material, adhesive wear will take place. Since the cold weld still is a relatively weak attachment, it is likely that the worn off fraction, called the wear debris, will detach at a later time [8]. The wear debris can also act as a protrusion, thus giving rise to abrasive wear [3, p. 310].

The wear of contacts is essentially proportional to applied load and to the sliding distance [8]. There is no apparent relation between the wear and the size of the contacts, however, which could appear as a counter intuitive result.

A result of the wear process is that the material is worn out, which can lead to failure of the contact. This is especially true if the contact is coated with a thin layer of a different material. If the coated layer is worn off, new conditions are present which can lead to various unforeseen reactions. In the case of OLTCs the timing of arc distinction can change, as an example [6].

Another result of the wear process is that the wear debris can lead to other new effects. For example the friction coefficient will rise once the amount of wear debris exceeds a certain threshold level when the interaction between the contact surfaces change. This phenomena is important for another type of mechanical wear, fretting, which will be described next.

### 2.3.4   Fretting and Thermal Deformations

Fretting is defined as the "accelerated surface damage occurring at the interface of contacting materials subjected to small oscillatory movements" [3, p. 179]. It is worth noting that this definition does not define the frequency range of the oscillatory movement, in contrast to the amplitude of the oscillation which should be small. Small in this case means that it is in the order of or smaller than $125\,\mu$m. Also, the source of the vibrations is unspecified.

Important parameters that characterize the fretting are the oscillation frequency and amplitude, the mechanical and electrical load of the contacts, the friction coefficient of the materials and various protection schemes such as lubricants [9].

In practice it is convenient to define two groups of fretting motion present in OLTCs, and the related sources thereof. The first group is one with small amplitude (often 0-50 $\mu$m) and relatively high frequency which is normally induced by mechanical vibrations originating from the AC-current flowing through the transformer [10]. The frequency is in this case $100\,$Hz. The second group is one with slightly higher amplitude and a much lower frequency. These motions often originates from temperature changes leading to different thermal expansion of different materials.

No complete theory to explain the characteristics of fretting has yet been found and it is usual that each new fretting case differs from previous ones. This is due to the many complex phenomena which can lead to fretting, and the many reaction trajectories which can give rise to essentially the same damage. It is therefore hard to extrapolate from studies performed under some given conditions to what will happen in situations with other conditions. There are some characteristics, however, that have been found to influence when and if fretting occurs, and these are the contact design and condition, as well as the environment in which the contact operates [3, p. 180].

The following is a description of a typical fretting process as is thought in the litterature today [3, p. 184]. It is illustrated in figure 4. As was discussed earlier in section 2.2 the surface of the contacts is typically very rough on a micro scale. The asperities from both sides of a contact pair will adhese, delaminate or microweld. The oscillatory movement will make these attachments shear and eventually break, depending on the amplitude of the movement in relation to the dimension of the asperities. Each detachment process incorporates the revealance of clean metallic surfaces which will quickly oxidize, both on the loose fragment and on the contact surface. With time there will be an accumulation of oxidized fragments between the contacts whose aggregated volume eventually will be greater than the available

space between the contacts. At this stage the fretting damage starts to cause really damaging effects on the contact resistance.

There is a possibility of creation of a very good connection between the contacts if two newly scraped areas form a contact spot before they oxidize. Thus, the contact resistance can sometimes decrease due to fretting. This is usually only a transition state, though, since the ongoing oscillatory movement will break the good connection again and the contact surfaces will be separated by the fragments, as described above.

### 2.3.5    Creep and Stress Relaxation

Creep and stress relaxation are two processes which take place under quite long time intervals. The effect of creep is essentially a lower resistance on its way to failure, while the opposite is true for stress relaxation. The effects of stress relaxation is an increase of resistance. Below, the phenomena are explained one at a time.

Creep, also called cold flow [3, p. 212], refers to the slow deformation of metals under load. Often it is sufficient to only take the instantaneous effect of an applied stress into account, such as elastic and plastic deformations. But sometimes failures can appear even though the product experiences stress well below its critical level. In these cases the failure is due to creep.

A typical creep curve, containing three stages, is shown in figure 5 [11]. A specimen is put under a constant load at a constant temperature. In the first stage, called primary creep and denoted A in the figure, the strain increases quickly from the instantaneous strain $\epsilon_0$, containing both elastic and plastic deformations. In the second stage B, called steady-state creep, the increase in strain over time is constant. This is the stage which is interesting for engineers because most deformations occur here and thus it is crucial to have understanding of this region to control the lifetime of a product [11]. In stage C, called tertiary creep, the strain again increases but now at an increasing rate leading to failure due to creep rupture.

But what happens when the material starts to creep? On the microscopic level it is the asperities of the contact surface which experience the highest strain that will creep first. The actual contact area will increase when the asperities are smoothed out, leading to a decrease in resistance during a transition period before stage C of figure 5 is reached. Furthermore, new contact spots will be formed as new asperities will come into contact [12].

As stated above, figure 5 depicts a scenario of constant temperature. But creep is also a function of temperature [11, 12]. This is due to the increased diffusion on the atomic scale at higher temperatures which then gives a higher creep rate for higher temperatures.
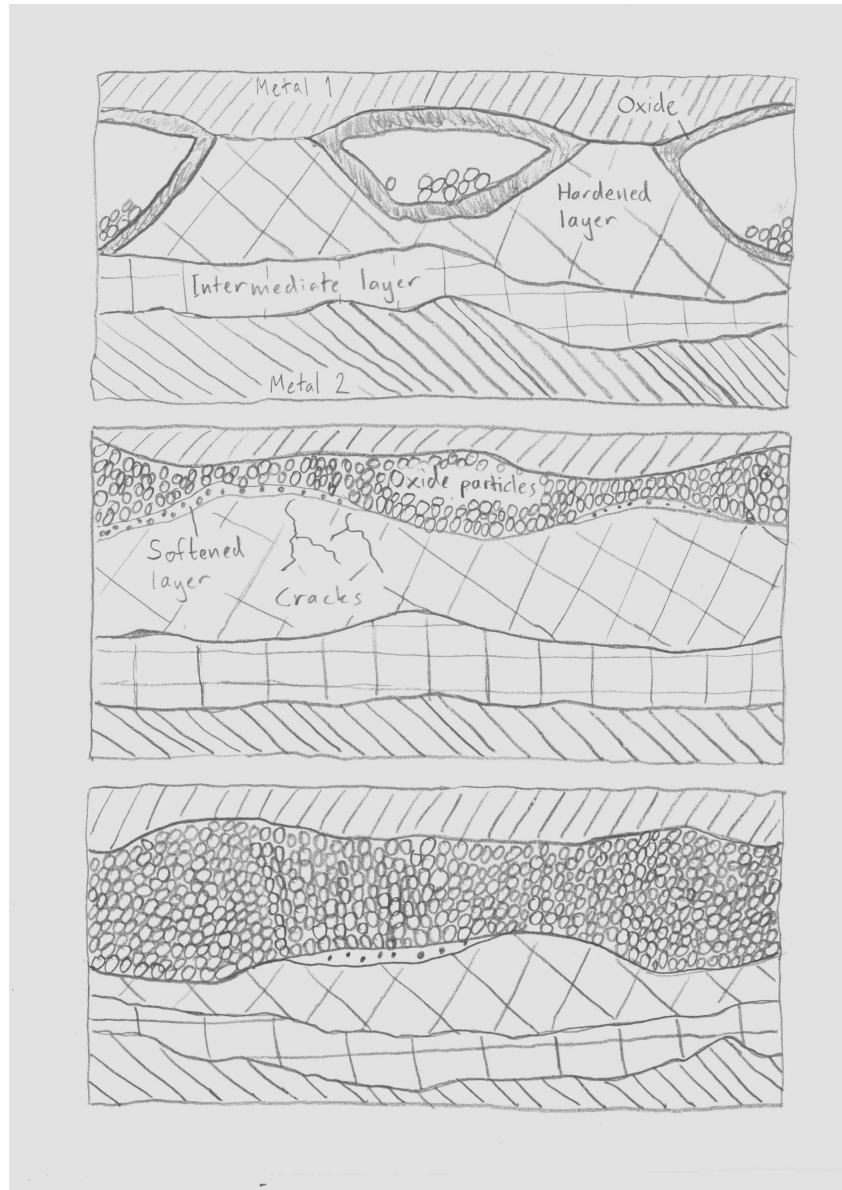
Figure 4: The development of fretting. The asperities from both sides of a contact pair will adhese, delaminate or microweld. The oscillatory movement will make these attachments shear and eventually break. Each detachment process reveal clean metallic surfaces which quickly oxidize, both on the loose fragment and on the contact surface. With time there will be an accumulation of oxidized fragments between the contacts whose aggregated volume eventually will be greater than the available space between the contacts. Based on [3, p. 185]
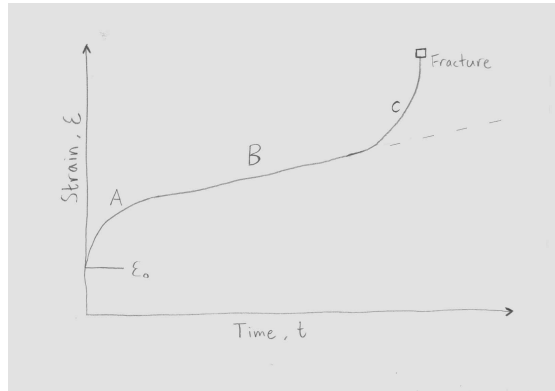
Figure 5: A typical creep curve. A specimen is put under a constant load at a constant temperature. Stage A is called primary creep, the strain increases quickly from the instantaneous strain $\epsilon_0$. In stage B, called steady-state creep, the increase in strain over time is constant. In stage C, called tertiary creep, the strain again increases but now at an increasing rate leading to failure due to creep rupture. Based on [11, p. 2].

Stress relaxation is, as stated above is a phenomenon which increases resistance. When contacts are operating under high mechanical stress for long periods of time the metal eventually relaxes, giving rise to stress relaxation [3, p. 212]. The relax process itself takes place on an atomic scale, where atoms spontaneously jump to more favorable locations. The rate of this process can be enhanced if current is flowing through the contact. When electrons, carrying some kinetic energy, collide with atoms in the contact region they may transfer some of its energy. This energy could be exactly what is needed for a dislocation to take place. It is said that there is an electron "wind" present [3, p. 213]. This view of the relaxation process makes it temperature dependent, since the probability of atomic jumps increase with temperature.

The macroscopic result of the relaxation of the contact material under stress is that the contact pressure decreases [3, p. 212]. As was stated in section 2.2, a lower contact pressure leads to a raise in resistance due to that there will be less actual contact area in the junction.

## 2.4 Accelerated Life Tests

Accelerated life tests (ALT) are tests designed to, in a short period of time, evaluate how a product will perform in its lifetime. This is achieved by exposing the product to excessive destructive conditions. Examples of this include elevated temperatures and power cycling, which will be discussed

further later on, as well as mechanical testing with an increased frequency of operation of the product and corrosive environment and so forth.

When designing an ALT, one has to use certain precausion. For the test to be valuable, one most accelerate the investigated failure mode, while not introducing failure modes that do not exist in real life applications. A time, effort and material saving approach can be to incorporate several excess stresses into a test and test several failure modes, but doing this also increases the risk of one of the modes dominating the others in the accelerated scenario but not in real applications.

Our aim with the project was to create a test that would incorporate the failure modes oxidation and coking. We used elevated temperatures and the Arrhenius relationship and temperature cycles. These concepts will now be discussed in further detail.

### 2.4.1 Arrhenius Relationship

A widely used model for accelerated testing is to use elevated temperatures and then calculate how the failure rate has increased according to the Arrhenius life relationship. The relationship is based on the Arrhenius rate law of a chemical reaction:

$$\text{rate} = A' \exp[-E/(kT)], \tag{3}$$

where $E$ is the activation energy of the reaction, $k$ is Boltzmann's constant, $T$ is absolute temperature and $A'$ is a characteristic constant depending on both the reaction itself as well as ambient conditions. The Arrhenius life relationship models a situation when failure is due to a chemical having reacted a certain critical amount, in our case oxidation of a metal.

$$\text{(critical amount)} = \text{(rate)(time to failure)}$$

giving

$$\text{(time to failure)} = \frac{\text{(critical amount)}}{\text{(rate)}}. \tag{4}$$

Combining equations (3) and ((4) gives the Arrhenius life relationship:

$$\tau = A \exp[E/(kT)] \tag{5}$$

where $\tau$ is the time to failure and $A$ is a characteristic constant depending on both the reaction itself as well as ambient conditions. Equation (5) predicts that the time to failure due to the chemical reaction is decreased as temperature is increased. This is known as the Arrhenius acceleration factor

$$K = \frac{\tau}{\tau'} = \exp\{(E/k)[(1/T) - (1/T')]\}, \tag{6}$$

the fraction between the time to failure according to equation (5) for two different temperatures $T$ and $T'$. The expected life time, $\tau$ of a specimen at temperature $T$ is thus $K$ times the expected life time, $\tau'$, at temperature $T'$. A rule of thumb is that the reaction rate doubles for each $10\,°C$ increase in temperature, but this does of course differ for different reactions since it depends on the activation energy. This decription of the Arrhenius life relationship is extracted from [13], chapter 9, where it is discussed in further detail.

### 2.4.2 Passivation and Temperature Cycling

As mentioned in section 2.3.1 oxidation can be limited by passivation. In an ALT, the accelerated rate of oxidation can lead to an initial oxidation in a temperature dependent rate, accelerated as described by equation (6), but then slowed down by a local passivation layer. [14] and [15] show the merits in cycling temperature, creating thermal deformations that counteract the passivation phenomenon. Even though the Arrhenius life relationship is a constant stress model, valid when temperature is constant, it can be necessary to expose the specimen to temperature cycling. In an electrical contact this can be achieved by current cycling, as in [14] and [15], or by changing the ambient temperature of the contact.

## 2.5 A Present Accelerated Aging Functional Life Test

A test which is currently used for development purposes to test the oxidation endurance of electrical contacts in the OLTC is the Accelerated Aging Functional Life (AAFL) test (sometimes reffered to as the Hopkinson test) [16, 17]. It has been developed by Philip J. Hopkinson[1] as a proposal to become a standardized type test for off-circuit tap changers in IEC 60214-1 [18].

The test is performed by keeping the tap changer in $130\,°C$ oil with a load of double the rated load current for 8 hours, followed by 16 hours of self cooling and no load. The test is performed during 30 days, which corresponds to 30 years of aging. There are two criteria for a contact to pass the test; the contact resistance increase from the first day to the last should be less than 25%, and the contact resistance should be stable at the end of the test [16, 17, 18].

---

[1]Philip J. Hopkinson is a Master of Science in System Science from Brooklyn Polytechnic Institute, an IEEE fellow and a very experienced Transformer Engineer. He is also the founder of HVOLT Inc. http://www.hvolt.com
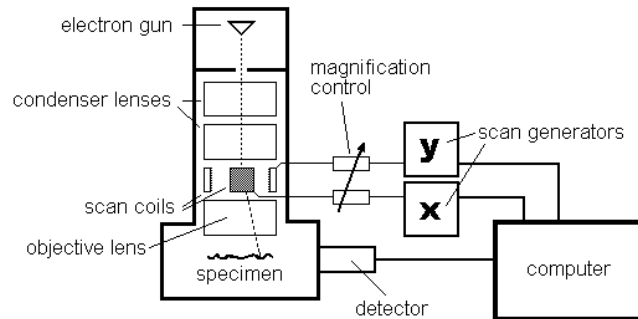
Figure 6: Schematic diagram of a scanning electron microscope [20, p.126]. A closer description of its functions is found in the text body.

## 2.6  Silver Iodide as Contact Material

Silver iodide is a metallic salt between the noble metal silver and the halegonide iodide. Silver has excellent electrical and thermal properties and is thus a popular material to use in contacts. Unfortunately it has a very high coefficent of friction, which leads to high wear when used in sliding contact applications, which are very common in OLTCs. By coating silver contacts with a thin layer of silver iodide the friction can be reduced dramatically. The setback is that the silver iodide coating, at least initially, increases the contact resistance. The resistance decreases when the contacts have been rubbed against each other and reaches a low and steady level after a number of repetitions. Visually, the silver iodide contacts are very light sensitive and blacken when exposed to light. When rubbed against each other, the black coating disappears where the contacts have been in physical contact, but the friction remains low. The silver iodide contacts thus have the favourable electrical properties of pure silver, but does not have the destructively high coefficient of friction of the silver contacts.[19]

## 2.7  Scanning Electron Microscopy

A schematic drawing of a scanning electron microscope (SEM) is shown in figure 6. An electron gun shoots an electron beam accelerated by applying a voltage, known as the accelerating voltage (also termed electron high tension, EHT [21]). The electron beam is narrowed and focused on a specimen by three lenses known as the condenser lenses and the objective lense. The intensity of the output from the objective lens is limited by an aperture. If nothing else is stated, the term aperture refers to the aperture of the objective

15

lens. The scan generators send signals to the scan coils so the coils generate magnetic field wich deflects electrons in the desired direction. A rectangular area of the specimen is horizontally scanned by fixing the y-direction and sweeping the x-direction, then slightly adjusting the y-direction and repeating, called a raster scan. Detectors then collects scattered electrons. There are electrons scattered in many different angles and energy spans and with different origins. These electrons carry different types of information why several different kinds of detectors and detector positions are used. A few of these will be discussed below. figure 6 show the schematic setup of a SEM.[20, pp. 126-128]

Secondary electrons are atomic electrons from the specimen that are inelastically scattered by the incoming electrons from the electron gun and thus ejected from the specimen [20, p. 128]. They can be collected by several different type of collectors with different energy ranges and advantages. SE2 is a secondary electron detector that collects secondary electrons from relatively deep inside the to sample [20, p. 144]. It is good for general purpose imaging [21]. InLens is a collector positioned above the objective lens where it collects secondary electrons emitted close to the optical axis and caught by the magnetic field of the lens [20, p. 136]. It is appropriate for topographic imaging [21].

Backscattered electrons are electrons from the electron gun that have entered the specimen and then been elastically scattered at an angel greater than 90 degrees, either by a singel event or by several events [20, p. 137]. EsB is a backscattered electron collector placed above the In-lens detector. EsB was first used to show compositional differences [22] and we were also thaught how to use it to gain topographic information.

Another way of collecting information with a SEM is energy-dispersive x-ray spectroscopy (EDX, also known as EDS and XEDS). Primary electrons entering the specimen may be eastically scattered by inner-shell electrons. The inner-shell electron then temporarily transitions to a higher energy level and, as it returns from its excited state, emitts a photon [20, p. 158]. The EDX collects the energy spectra of emitted photons, and by comparing these to the energy spectras of inatomic transitions for the different elements, a compositional mapping can be made in the area exposed to the electron beam.

# 3  Oxidation Endurance Test of OLTC Contacts

To be able to distinguish between good and bad contact solutions for the OLTC during its lifespan it is needed to perform accelerated life testing which simulates contact behavior in real life applications, but in a shorter period of time. Economically it is preferable with a short test, but the test might become decreasingly accurate the shorter it is, making a compromise necessary. Also, it can be difficult to realize a high acceleration factor in practice, imposing a natural lower limit on the test time.

The main electrical aging parameter of OLTC contacts is resistance. As described in the theory section, a higher resistance leads to greater heat generation in the contact which leads to more aging and eventually failure of the contact. It was also described in sections 2.3.1 and 2.3.2 that two major failure modes are oxidation and coking (which is initiated by contact oxidation). The purpose of the present test method is to distinguish between good and bad contact solutions regarding resistance runaway due to oxidation and coking.

In short, the test is designed to...

- be able to test all moving OLTC contacts in oil,

- correspond to 30 years of aging,

- take the failure modes oxidation, coking and thermal deformation into account,

- let the contacts experience thermal deformations as in a typical real life situation,

- automate the test to an as large degree as possible to minimize work load and increase data quantity and integrity,

- simulate the worst possible scenario for OLTCs with respect to the above points.

The AAFL test, described in section 2.5, will be used as the base of the development of the present test since it is already used in practice and since its purpose and goal are close to the ones specified above. In the next section the AAFL test will be discussed and in the following sections the present test will be developed, leading forward to a proposal of a general testing procedure in section 3.5.

## 3.1   Possible Improvements of the AAFL Test

The AAFL test is undoubtfully a good test to evaluate the long term oxidation endurance of tap changer contacts, but there are a number of problems with the test which could make it unsuitable as a standardized test for OLTCs. Some of these were pointed out at a recent meeting of the IEEE/PES Transformers Committee [23]. In the following these problems will be discussed together with proposed possible solutions.

First, the theoretical motivation of the currently proposed AAFL test is not complete. The level of the oil temperature and the load current is adequately motivated, but not the cycling of the oil temperature. It would probably be a much less efficient test, maybe even worthless, without temperature cycling. But what motivates one cycle per day? Why not one cycle per week? Another problem is regarding the temperature difference during a temperature cycle. With the currently proposed test this temperature difference is arbitrary due to the spontaneous cool down which is dependent on oil volume, container dimensions and surrounding temperature.

Second, the AAFL test simulates a scenario where the OLTC contacts are stationary for the full 30 years. ABB's service instructions for tap changers are that the tap changer should be operated from end-position to end-position at least once each service stop. A service interval is typically 5-7 years, meaning that the OLTC at least is operated at four occasions during its lifetime of 30 years.

Third, the oil quality and volume are unspecified. Most important in this respect is probably the question of oxygen concentration during the test. It is of course desirable to mimic real life conditions of the oil in a power transformer. To define what this means is not an easy task, though. Furthermore, the outcome of the test is probably dependent of the oil flow within the container.

Forth, the criteria to pass the test are dubious. Regarding the first criterion (increase in resistance less than 25%) it is susceptible to arbitrary preparations of the contacts. A high initial resistance can "save" a contact from failing the test, essentially making the rest of the test unimportant. Some contacts record high values during the first few days, after which the resistance decreases to a stable or only slightly increasing value. Regarding the second criterion ("Resistance change has stabilized and is not continuing to rise." [16, p. 5]) one can first ask what stable means? It is also quite expected that the resistance increases over time. Imagine two contacts, one with quite high resistance and one with much lower. The first stays at a high, even level for the entire test period. The second records its lowest resistance the first day which then increases at a constant rate to 25% its initial

value over the 30 days, but still has lower resistance than the first one. The first contact will pass the test, the second will not, even though it has lower resistance at all times. This is a problem that need attention.

## 3.2   Reference Case

To be able to theoretically design an aging test, a reference case against which the aging is compared needs to be defined. It is supposed to mimic the operation conditions of OLTCs in as general terms as possible to be applicable on as many OLTCs as possible. The most crucial reference temperature to define is the one at the contact spot. This is where the temperature reaches its maximum in the OLTC and it is thus where the oxidation will be most prominent.

The temperature at the contact spot is primarily a sum of contributions from three different sources. First, there is the transformer oil temperature $T_{o,ref}$ which will be the base. The temperature of the contact spot will never go below this value. Second, the contact bulk temperature $\Delta T_{b/o,ref}$ will be elevated when it is under load, and third, the contact spot itself will have an increase in temperature $\Delta T_{s/b,ref}$ than the contact bulk due to the finite dissipation of heat.

We follow the AAFL test [16] when it comes to the working environment of the OLTC. The oil temperature of the transformer is thus taken as $T_{o,ref} = 75\,°\text{C}$. In contrast to the AAFL test, though, we model a seasonal temperature variation of $50\,°\text{C}$, which is assumed to be propagated with a factor of one to the oil temperature.

From the IEC standardized temperature rise test [4, p. 35] it is given that with a current of 1.2 times the rated load current the bulk temperature cannot rise more than $20\,°\text{C}$ over the ambient temperature. Using equation (1) of section 2.2 it is then possible to calculate the maximum bulk temperature rise over the oil temperature $\Delta T_{b/o}$ at the rated current. First the proportionality constant is decided:

$$
\begin{aligned}
\Delta T_{b/o} &= c\,(1.2 I_r)^{1.6} = \Delta T_{tr/a}, \\
\implies c &= \frac{\Delta T_{tr/a}}{(1.2 I_r)^{1.6}}.
\end{aligned}
\tag{7}
$$

Here $I_r$ is the rated load current and $\Delta T_{tr/a}$ is the maximum allowed temperature rise over the ambient temperature, $20\,°\text{C}$. The maximum bulk tem-

perature rise at the rated current is then:

$$\Delta T_{b/o,max} = c\,(I_r)^{1.6} = \Delta T_{tr/a,max}\left(\frac{1}{1.2}\right)^{1.6} = 20\,°\mathrm{C}\left(\frac{1}{1.2}\right)^{1.6} = 14.9\,°\mathrm{C}.$$
(8)

The contact bulk temperature rise over the oil temperature will be taken as $\Delta T_{b/o,ref} = 15\,°\mathrm{C}$. It is here worth noting that the AAFL test, since it assumes a higher bulk rise than this, actually violates the standardized temperature rise test.

The super temperature rise over the bulk will in the reference case be taken as $\Delta T_{s/b,ref} = 7\,°\mathrm{C}$. When using equation (2) of section 2.2, with $25\,\mathrm{mV}$ as the contact voltage drop at rated current[2], this is the acquired result.

To summarize, the temperature of the contact spot at which the contact is modeled to age during 30 years in this reference case is:

$$T_{c,ref} = T_{o,ref} + \Delta T_{b/o,ref} + \Delta T_{s/b,ref} = 75 + 15 + 7\,°\mathrm{C} = 97\,°\mathrm{C}.$$
(9)

It is against this temperature that the aging of the test object will be compared.

## 3.3   Controllable Parameters

To be able to perform the test defined above an analysis has to be carried out about which possibilities that are available to realize the test. In other words, the variable parameters that exist need to be found, and this will be done here. In the next section these parameters will then be quantitatively calibrated to reach the defined goals of the test.

The test is designed to simulate the real life conditions of OLTCs as closely as possible. It is therefore suggested that the test will be performed in regular transformer oil and that the OLTC will be put under load similar to normal operation. To accelerate the wear on the OLTC, some parameters has to be exaggerated though. The oil temperature and the load current appear as natural parameters available to control. They will be denoted $T_o$ and $I$, respectively.

It is also possible to cycle both the oil temperature and the load current, and the number of such cycles per day are denoted $N_o$ and $N_I$, respectively. The amplitude of the temperature cycle can also be controlled, it will be

---

[2]Applied to the reference tap changer we evaluate the test on, with a rated current of $600\,\mathrm{A}$ and 4 individual contacts on each contact arm, this corresponds to a total contact resistances of $40\,\mu\Omega$ for the entire arm.

Table 1: Controllable parameters together with their calibrated values to be able to perform the defined test.

| | Parameter | Value |
|---|---|---|
| $T_o$ | Maximum oil temperature | $120\,°C$ |
| $I$ | Maximum load current | $1\,200\,A$ |
| $N_o$ | Number of oil temperature cycles per day | 1 |
| $\Delta T_o$ | Amplitude of oil temperature cycles | $50\,°C$ |
| $N_I$ | Number of current cycles per day | 31 |
| $\tau_I$ | Time at maximum load current per cycle | $26\,min$ |
| $\tau_o$ | Time at maximum oil temperature per cycle | $18\,h$ |
| $[O_2]$ | Oil oxygen concentration | Uncontrolled |

denoted $\Delta T_o$. The amplitude of the current cycle is not considered a controllable parameter since this would require it to be controlled by more advanced electronics than a simple switch. Moreover, the duty cycle of the cycling can be chosen freely by the test designer. The time spent at the maximum value is denoted $\tau_{o,max}$ and $\tau_{I,max}$, respectively.

Since we are taking the oxidation failure mode into account it is also important to control the oxygen concentration of the oil, which will be denoted $[O_2]$.

This finishes the analysis of controllable parameters. To summarize, we have found that the time at maximum, the number of cycles and the duty cycle are controllable parameters for the oil temperature and the load current, as well as the amplitude of the temperature cycle. It is also possible to control the oxygen concentration of the oil. This gives a total of eight controllable parameters to design the test. In the next step they are to be defined quantitatively.

## 3.4   Calibration of Controllable Parameters

The seven parameters available for control which were found in the previous section are shown in table 1. Shown in this table are also their calibrated value, which will be deduced in the following section.

There are three failure modes that are to be calibrated, as was stated in section 3. These are oxidation, coking and thermal deformations. From the controllable parameters that were found in the previous section this will be possible, and further, the parameters can be assigned to the calibration of individual phenomena. The calibration of oxidation and coking will be performed through the high temperatures and the time spent at these tem-

peratures. This is due to the acceleration stemming from the Arrhenius equation, as was explained in section 2.4.1. The calibration of thermal deformations, on the other hand, will be performed with the number of cycles and the amplitude of temperature differences of the cycles.

The deduction is started with parameters which are essentially determined by reasons that the test designer cannot influence. The optimal choice is therefore to fix the parameter at an extreme of the possible interval of parameter choice. To design a test one sometimes needs to compromise between what could yield an optimized test regarding some variable, and what is practical.

In the AAFL test, the test time is 30 days. As previously mentioned, to shorten the test time might give less trustful results, but 30 days is already a long time. We thus aim to keep the test length to 30 days since it is a time that has been deemed acceptable before. Each day of simulated aging should thus correspond to one year of real life aging. This means that during the 24 hours of a day $24 \cdot 365 = 8760$ hours of corresponding real life aging should be reached.

### 3.4.1   Maximum Oil Temperature $T_o$

The acceleration of the aging is largely dependent on the temperature of the contact spot, as was explained in section 2.4, and to reach a high acceleration it is thus desirable to have a high oil temperature. An upper bound is however imposed in practice due to the risk of fire, which increases for higher oil temperatures. The flash point of the used oil is $140\,°C$. Under prevailing safety regulations at ABB Ludvika the highest oil temperature that can be kept continuously over nights and week-ends is $120\,°C$, so this is the temperature the test will be performed at.

### 3.4.2   Maximum Load Current $I$

The level of the maximum load current accelerates the aging by two mechanisms, which essentially have the same source: generation of heat by $P = UI$. The two mechanisms are ($i$) an increase of the contact bulk temperature, and ($ii$) an increase of the contact spot temperature over the bulk temperature.

In the AAFL test the load current is set to two times the rated load current. There exist both benefits and drawbacks with this choice. One benefit is that the current does not differ that much from normal working conditions, which increases the credibility of the test as a simulation of real world aging. It is important to minimize the risk of stimulating other failure modes than under normal operation and a good way to do this is to not

diverge too far from normal operation loads. Another benefit is that each contact design gets tested in proportion to its stated electrical properties, in this case the rated load current. A drawback of this, on the other hand, is that different contact designs get tested with a different acceleration factor. Since the acceleration is exponentially dependent of the temperature, also small differences in temperature that are sustained for long periods of time give rise to large differences in corresponding aging time.

In the present test we have chosen to follow the AAFL test and use twice the rated load current. In this case, with the tap selector that is used and will be described in section 3.7, this means $I = 1200\,\text{A}$.

The maximum bulk temperature rise is calculated in the same way as in section 3.2 using equations (1), (7) and (8). The maximum bulk temperature rise at twice the rated current is then:

$$\Delta T_{b/o} = c\,(2I_r)^{1.6} = \Delta T_{tr/a,max}\left(\frac{2}{1.2}\right)^{1.6} = 20\,^{\circ}\text{C}\left(\frac{2}{1.2}\right)^{1.6} = 45.3\,^{\circ}\text{C}. \quad (10)$$

This will be used as the theoretical temperature rise of the contact bulk over the oil temperature.

### 3.4.3  Number Of Oil Cycles and Amplitude Of Oil Temperature Cycles Per Day $N_o$ and $\Delta T_o$

The primary reason for oil temperature cycling is to induce thermal deformation to break up the $a$-spots (see section 2.2). This is important to mimic real life conditions as closely as possible, where thermal fluctuations will make contacts spots break and reform with likely long-term effects on the resistance properties of the contact. The cycling of oil temperature will be used to simulate thermal deformations on the contact spot due to temperature changes over the four seasons. Since each day of testing corresponds to one year of aging, one oil temperature cycle should be performed per day, as in the AAFL test. A reasonable temperature difference over one year is $50\,^{\circ}\text{C}$, why we choose to bring the oil temperature down this much. Thus $N_o = 1$ and $\Delta T_o = 50\,^{\circ}\text{C}$.

### 3.4.4  Number of current cycles per day $N_I$

While the cycling of oil temperature corresponds to seasonal variations in ambient temperature, the cycling of load current will simulate daily variations. The source of these variations are twofold: ($i$) variations in ambient temperature over the day and ($ii$) variations in load current over the day giving rise to varying contact bulk temperature. The variations in ambient
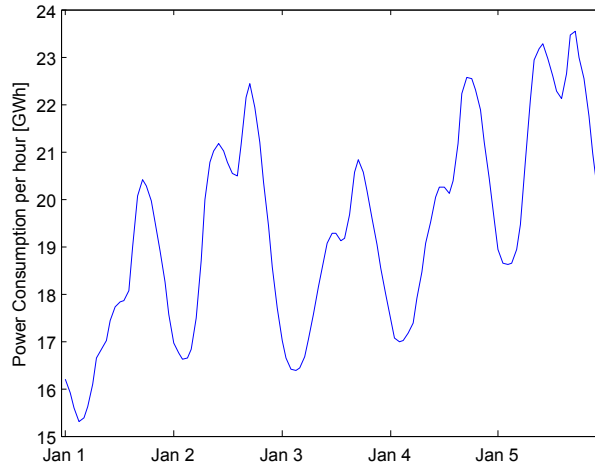
Figure 7: Consumed power per hour in the Swedish power grid during the first five days of 2009. Data from [24]. It was used for calibrating the daily power deviations an OLTC experiences.

temperature over the course of one day needs to propagate through the oil to the contact to have any effect. Data showing in what degree this takes place has not been found and is therefore neglected in the present thesis, and we therefore focus solely on the variations in load current to calibrate this parameter.

To get an estimate of how much the current varies in the power grid over a day data from Svenska Kraftnät have been analyzed [24]. In figure 7 the consumed power during January 1 to 5 can be seen as an example of how the current varies during the course of a few days. If one makes the simplifying assumptions that the same OLTCs are used throughout the day and that the voltage regulation of these are constant, the current variations over the day can be approximated. Over the 365 days during 2009 the mean ratio between the minimum and the maximum consumed power was 0.741, varying from 0.728 to 0.773. From $P = UI$ and the assumption made that the voltage is constant, it follows that also the current in the grid varies 26% over a day. The mean consumption was 62 % of the top consumption [24]. We rounded the mean value upwards to 70 % of the rated current (indirectly assuming that the grid at the maximum point might have been run at a higher capacity than rated). The mean maximum consumption thus became 80 % and the mean minimum consumption 60 %[3].

Again, we use the assumption from the IEC standard [4, p. 35] that the

---

[3]$\frac{59.6}{80.4} = 0.741$, $\frac{59.6+80.4}{2} = 70$

contact bulk temperature rise is $20\,°\mathrm{C}$ over the oil temperature at a load of 1.2 times the rated current is used. Moreover, it is assumed that the OLTC is working at its rated load current during the maximum power outtake each day. From this follows, again using equations (1), (7) and (8), that the contact bulk temperature changes

$$
\begin{aligned}
\Delta T_{b,day} & = T_{max} - T_{min} = c(0.8I_r)^{1.6} - c(0.6I_r)^{1.6} = cI_r^{1.6}(0.8^{1.6} - 0.6^{1.6}) = \\
& = \frac{\Delta T_{tr/a}}{(1.2I_r)^{1.6}}I_r^{1.6}(0.8^{1.6} - 0.6^{1.6}) = \frac{\Delta T_{tr/a}}{1.2^{1.6}}(0.8^{1.6} - 0.6^{1.6}) = \\
& = \frac{20\,°\mathrm{C}}{1.2^{1.6}}(0.8^{1.6} - 0.6^{1.6}) = 3.9\,°\mathrm{C}
\end{aligned}
$$

each day.

As was already calculated above in equation (10) the contact bulk temperature changes by $\Delta T_{b,test} = 45.3\,°\mathrm{C}$ when the load current goes from zero to twice the rated load current, as it will in this test design.

Now, the calibration target is the thermal deformation length

$$
\Delta l = l_0 \alpha \Delta T,
$$

where $l_0$ is the original length and $\alpha$ is a material constant. Since this is a linear equation in $\Delta l$ and $\Delta T$, it follows that the sum of temperature differences over a year in real life operation should equal the sum of temperature differences during one day of cycling in the test. Thus, the number of cycles should be

$$
N_I = \frac{365 \cdot 3.9\,°\mathrm{C}}{45.3\,°\mathrm{C}} = 31.[4]
$$

### 3.4.5    Time at maximum load current per cycle $\tau_I$

It is now time to calibrate the aging regarding the oxidation and coking. It has already been decided that the test will run in $120\,°\mathrm{C}$ oil and that the contact bulk temperature will rise $45.3\,°\mathrm{C}$ above this value. In the contact spot, there will be an additional temperature increase due to the current, and this is where the aging of interest takes place.

From equation (2) in section 2.2 we can calculate the supertemperature, that is the temperature of the contact spot, if we know the contact bulk temperature and the voltage drop over the contact. Once again we take

---

[4]When we did our deduction for the evaluation test we used the more exact numbers 80,4 % and 59,6 % to calculate $\Delta T_{b,day}$ and then got $N_I = 32$. This difference should be negligable.
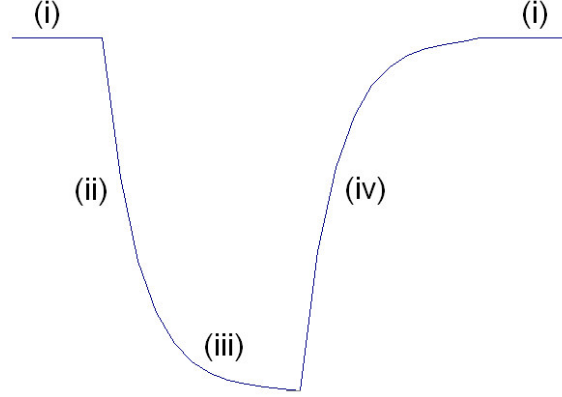
Figure 8: The different temperature regions of a power cycle, $(i)$ at maximum temperature, $(ii)$ bulk cooling, $(iii)$ at oil temperature, and $(iv)$ bulk warming.

$25\,\mathrm{mV}$ as the contact drop at rated current. It then follows that the maximum temperature in the contact spot at twice the rated current is

$$
\begin{aligned}
T_c &= \sqrt{\frac{U^2}{4L} + T_b^2} = \sqrt{\frac{50\,\mathrm{mV}^2}{4 \cdot 2.45 \cdot 10^{-8}\,\mathrm{V^2 K^{-2}}} + (273.15 + 120 + 45.3\,\mathrm{K})^2} = \\
&= 466.63\,\mathrm{K} = 193.5\,^\circ\mathrm{C}.
\end{aligned}
$$

The corresponding super temperature is $\Delta T_{s/b} = 28.2\,^\circ\mathrm{C}$.

Now, there are in principle four temperature regions for the contact spot which are occupied at different time intervals during the aging period. These are shown schematically in figure 8 and can be characterized as $(i)$ at maximum temperature, $(ii)$ bulk cooling, $(iii)$ at oil temperature, and $(iv)$ bulk warming. The acceleration factor for each of these regions are now to be determined, so that the total accelerated aging can be calculated. The reference temperature against which the contact spot temperatures of these regions will be compared, calculated in equation (9) of section 3.2, is $T_{c,ref} = 97\,^\circ\mathrm{C}$.

$(i)$ **- At maximum temperature**   The maximum temperature has previously been deduced to be:

$$
T_{c,i} = T_o + \Delta T_{b/o} + \Delta T_{s/b} = 120 + 45.3 + 28.2\,^\circ\mathrm{C} = 193.5\,^\circ\mathrm{C}.
$$

The corresponding acceleration factor, with a doubled reaction rate each $10\,^\circ\mathrm{C}$[5] of increased temperature from the rule of thumb for the Arrhenius

---

[5]In [25] a study of oxidation of copper films was performed that indicated that, at least for copper, the reaction rate might infact be doubled for slightly lower temperature

relationship in section 2.4.1, is then:

$$a_i = 2^{\frac{T_{c,i} - T_{c,ref}}{10\,^\circ\mathrm{C}}} = 2^{\frac{193.5\,^\circ\mathrm{C} - 97\,^\circ\mathrm{C}}{10\,^\circ\mathrm{C}}} = 803.$$

($ii$) **- Bulk cooling**   When the contact bulk cools it will decay exponentially towards the oil temperature. Assuming that the super temperature disappears immediately, and that the cooling is said to be ended after time $\tau_{ii}$ when 90% is cooled, the following set of equations describe our scenario, where $\Delta T_{c/o}$ denotes the contact temperature rise over oil temperature:

$$
\begin{aligned}
\Delta T_{c/o}(t) &= ae^{-bt} \\
\Delta T_{c/o}(0) &= \Delta T_{b/o} \\
\Delta T_{c/o}(\tau_{ii}) &= 0.1\Delta T_{b/o}
\end{aligned}
$$

where $a$ and $b$ are constants. From this it follows that

$$\Delta T_{c/o}(t) = \Delta T_{b/o} e^{-\frac{t\ln 10}{\tau_{ii}}}.$$

The mean temperature during the cooling period $\tau_{ii}$ is

$$\Delta T_{c/o,ii} = \frac{\Delta T_{b/o}}{\tau_{ii}} \int_0^{\tau_{ii}} e^{-\frac{t\ln 10}{\tau_{ii}}}\,\mathrm{d}x = \frac{0.9\Delta T_{b/o}}{\ln 10} = \frac{0.9 \cdot 45.3}{\ln 10} = 17.7\,^\circ\mathrm{C}$$

The mean contact temperature during the cooling is thus

$$T_{c,ii} = T_o + \Delta T_{c/o,ii} = 120 + 17.7 = 138\,^\circ\mathrm{C}$$

Using this mean temperature, an approximate acceleration factor of the cooling period can be calculated as

$$a_{ii} = 2^{\frac{T_{c,ii} - T_{c,ref}}{10}} = 2^{\frac{138\,^\circ\mathrm{C} - 97\,^\circ\mathrm{C}}{10}} = 17.$$

($iii$) **- At oil temperature**   The acceleration factor can be immediately calculated as

$$a_{iii} = 2^{\frac{T_{c,iii} - T_{c,ref}}{10}} = 2^{\frac{120\,^\circ\mathrm{C} - 97\,^\circ\mathrm{C}}{10}} = 4.9$$

increases in the relevant temperature interval. Since $10\,^\circ\mathrm{C}$ is a well established number, and also used in the AAFL test, we decided to use it for our calculations, but feeling reassured that the number is not higher.

$(iv)$ **- Bulk warming**    Following a derivation similar to the one performed in $(ii)$ above, but instead with the set of equations

$$
\begin{aligned}
\Delta T_{c/o}(t) &= a(1 - e^{-bt}) \\
\Delta T_{c/o}(0) &= 0 \\
\Delta T_{c/o}(\tau_{iv}) &= 0.9(\Delta T_{b/o} + \Delta T_{s/b})
\end{aligned}
$$

giving

$$
\Delta T_{c/o}(t) = (\Delta T_{b/o} + \Delta T_{s/b})(1 - e^{-\frac{\ln 10}{\tau_{iv}}t})
$$

one acquires the mean temperature during warming as

$$
\Delta T_{c/o,iv} = (\Delta T_{b/o} + \Delta T_{s/b})\left(1 - \frac{0.9}{\ln 10}\right) = (45.3 + 28.2)(0.609) = 44.8\,°\text{C}.
$$

The mean contact temperature during the heating is thus

$$
T_{c,iv} = T_o + \Delta T_{c/o,iv} = 120 + 44.8 = 164.8\,°\text{C}
$$

The load current is on during this period, so that the super temperature contributes to the aging. The acceleration factor of the warming period can then be calculated as

$$
a_{iv} = 2^{\frac{T_{c,iv} - T_{c,ref}}{10}} = 2^{\frac{164.8\,°\text{C} - 97\,°\text{C}}{10}} = 110.
$$

So the acceleration factors at the four temperature regions of figure 8 are now known. But how long time is spent at each region? This is to some extent up to the test designer to decide.

Heuristic time intervals of the cooling and warming are $\tau_{ii} = \tau_{iv} = 5\,\text{min}$. To be on the safe side that the low temperature (oil temperature) is actually reached during cooling, the time spent here is also set to $\tau_{iii} = 5\,\text{min}$.

The remainder of the time is spent at maximum contact spot temperature. Since 31 cycles are to be completed[6], this means that $30 \cdot 5\,\text{min} = 2.5\,\text{h}$ are spent in the temperature intervals $\tau_{ii-iv}$ each day. They correspond to an simulated aging of $42\,\text{h}$, $12\,\text{h}$ and $274\,\text{h}$ respectively, totalling $328\,\text{h}$.

As one year is $8760\,\text{h}$, the total time at maximum current must correspond to $8760 - 328 = 8432\,\text{h}$. With its acceleration factor of 803, the total time at maximum temperature becomes

$$
\frac{8432}{803}\,\text{h} = 10.5\,\text{h}.
$$

---

[6]By 31 cycles we mean 31 power peaks and thus 30 powerless periods in between.

Table 2: Contribution to aging during one day of testing from the four temperature regions in figure 8. One year contains $24 \cdot 365 = 8760$ hours.

|  | Acceleration factor | Time spent [h] | Corresponding aged time [h] |
|---|---|---|---|
| $(i)$ | 803 | 10.5 | 8 431 |
| $(ii)$ | 17.7 | 2.5 | 42 |
| $(iii)$ | 4.9 | 2.5 | 12 |
| $(iv)$ | 110 | 2.5 | 275 |
| In total: |  | 18 | 8 760 |

The total time at maximum load current is the sum between the time spent in $(i)$ and $(iv)$, $10.5 + 2.5 = 13\,\text{h}$. This gives a total time at maximum power of each cycle

$$\tau_I = \frac{13}{30}\,\text{h} = 26\,\text{min}.$$

A summary of the results acquired above can be seen in table 2.

### 3.4.6   Time at maximum oil temperature per cycle $\tau_o$

The total time needed at maximum temperature is thus $10.5 + 3 \cdot 2,5 = 18\,\text{hours}$. The remaining 6 hours of the day may be used to cool and reheat the object the $50\,°\text{C}$ specified in 3.4.3.

### 3.4.7   Oil oxygen concentration [O$_2$]

The oxygen concentration of the oil will in this test be left uncontrolled. It is thought to follow the levels of a typical transformer oil naturally, which means it starts at 10 000 ppm by volume, increases to 20 000 ppm during the second year and saturates at 30 000 ppm during the following years. Gas analysis will be performed during the test to verify this assumption.

An option could have been to oxygenize the oil by bubbling air through the oil. This option is rejected, however, due to the risk of submitting excess volumes of oxygen. In such a case, the test object could oxidize too quickly, making the test worthless.

## 3.5   Working-proposal of an Oxidation Endurance Test

As was seen in section 3.1 there are some problems remaining with the AAFL test as it is designed today. The following is a proposal of a test method, building on the AAFL test, designed to coupe with some of these problems.

The proposed test should be performed as follows. Keep the OLTC in 120 °C transformer oil under load of double the rated load current for 18 hours, whereafter the load is turned off and the oil is actively cooled to 70 °C and then heated again to reach 120 °C after 6 hours. Cycle the current by turning it off for 10 minutes during 30 equally separated intervals during the load period. Run the test for 30 consecutive days, corresponds to 30 years of product life. Operate the OLTC in accordance with relevant maintenance instructions at times corresponding to real life service intervals.

The criteria to pass the test will be discussed in section 3.8 and in the discussion section 6 of the thesis.

## 3.6   How the Proposed Test is Realized

It is here presented how the test described in section 3.4 above was realized in practice. Beyond the obvious goal to realize the proposed parameter values, security measures need to be taken, due to the inherent risk of fire during the test. Moreover, since the test is designed to be highly automated, control hardware as well as software need to be developed. In our case, we have used LabView.

Four devices are used to regulate the parameter values of the test; a measurement current source, a load current source, an oil warming system and an oil cooling system. In addition to this a measurement system is implemented to monitor the changes of the oil and contacts. A schematic image depicting these five fundamental parts of the test is shown in figure 9.

The test needs to be manually operated once each morning and once each afternoon. In the morning the load (aging) current is to be disconnected from the test object to be replaced by the measurement current. This is when the oil temperature cycle begins, during which resistance and temperature measurements are carried out automatically. In the afternoon the opposite is performed: The measurement current is disconnected and is replaced by the load current. During the night the load current is then cycled automatically.

In the following is presented firstly the electrical (hardware) realization of the test together with the security solution, since these naturally intertwine. Secondly, the software solution is sketched out in general terms.

### 3.6.1   Hardware Solution

The purpose of the hardware solution is to be able to control the parameters of the test in a flexible, safe and straight forward fashion. The solution is
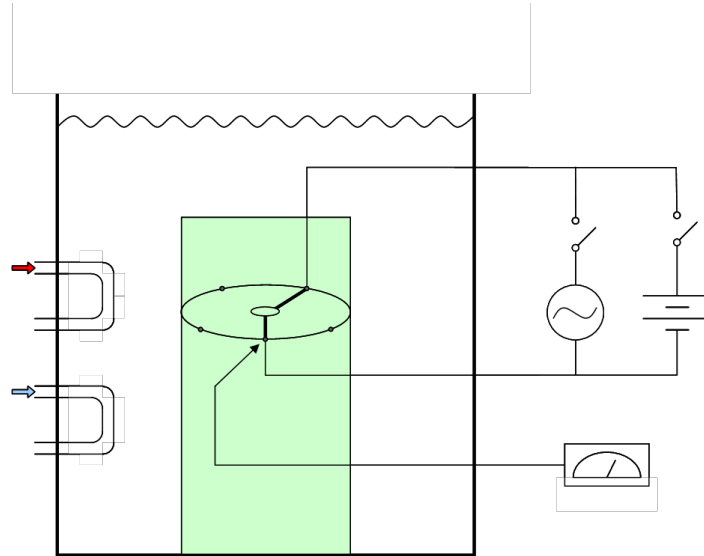
Figure 9: Schematic representation of the five fundamental parts in realizing the test. In the middle is the tank filled with oil wherein the test object is placed. On the left are the oil warming and cooling systems. On the top right are the two different current sources; the measurement and load currents. On the bottom right is the measurement system which monitors the contacts.

mainly divided in three parts: a security part, a control part and a measurement part. An overview of the hardware solution is given in figure 10.

To minimize the risk of fire two security systems have been implemented in the test design. The first is a temperature switch of the oil temperature at the surface, which is where the highest temperature is reached and oxygen is readily available and thus where a fire would initialize. If the surface temperature exceeds 130 °C the test is interrupted automatically. The second security system is an oil level switch. In case the oil level declines, for example if a leakage of the tank arises, the current carrying contacts will eventually come closer to the surface. Local maxima of the oil temperature might then reach the flash point, without the temperature switch detecting it. The test is therefore also interrupted automatically would the oil decline below a level deemed as secure.

During the AAFL tests that have been performed previously at ABB Ludvika an oil temperature of 130 °C have been used, but the oil was only kept at this temperature during daytime when it could be monitored. The change, compared with the AAFL test, to perform the test at 10 °C lower temperature during night time turns out to give approximately the same
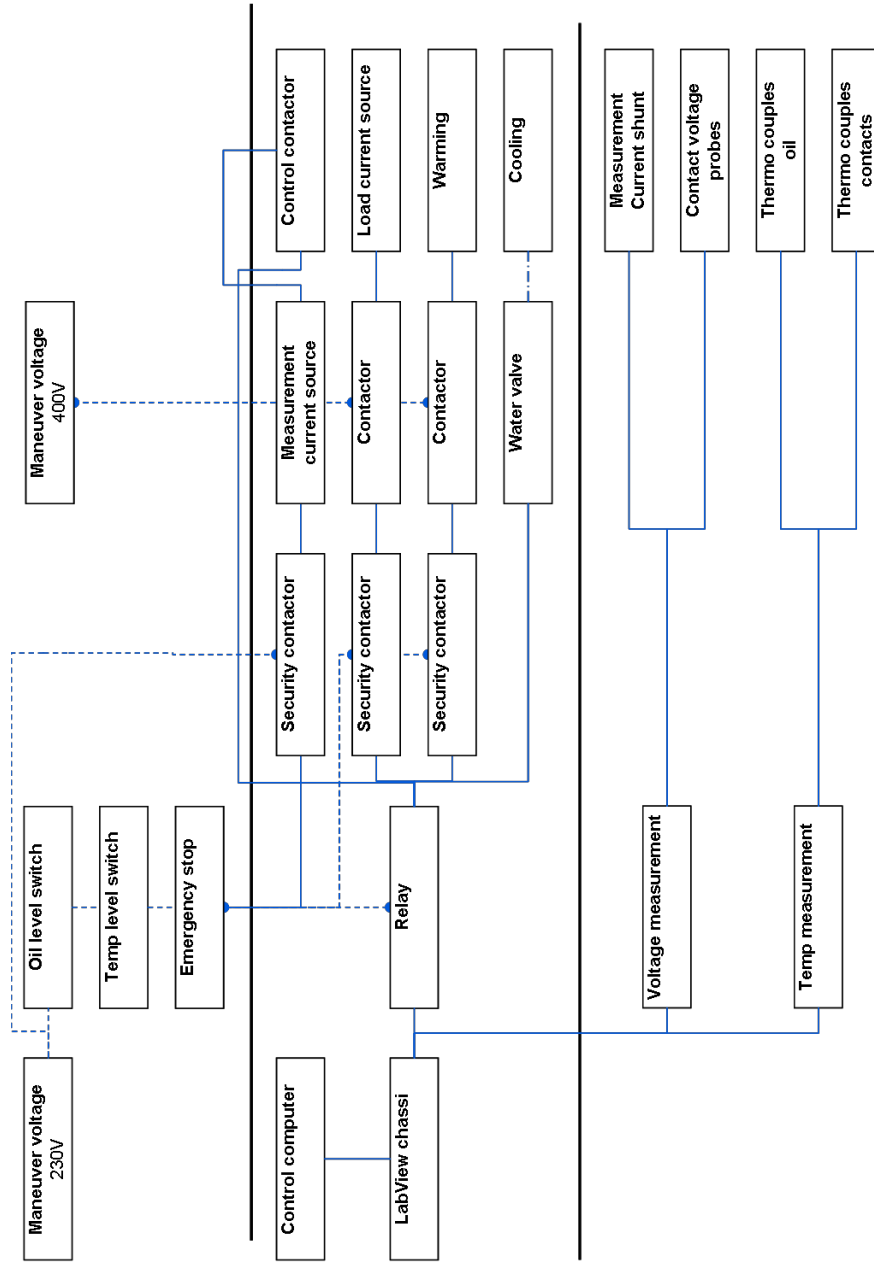
Figure 10: Schematic representation of the hardware solution to realize the test. The solution consists mainly of tree parts: the security solution at the top, the control solution in the middle and the measurement solution at the bottom. Dashed lines represent supply voltages, filled lines other electrical connections and the dash-dotted line a water hose.

aging acceleration per day. The aging acceleration per unit of time halves, but it is kept at the maximum temperature during approximately the double amount of time, which thus yields the same acceleration factor.

There is also a manual emergency stop mounted on the container in which the test is performed. As can be seen in figure 10 the maneuver voltage goes through the three security steps in series, meaning that if any one of these security steps activates, the supply voltage of the following components will be lost.

In the middle of figure 10, the control part, a quite complex system of relays, contactors and test influencing devices can be seen. The complexity arises from the combination of the security system with the control task. The overall function of this middle part is that the four parameter regulation devices are to be controlled from the computer. To the computer a four channel relay is connected. Each of these can then turn the regulation devices on or off.

The load (aging) current is $1200\,\mathrm{A}$, twice the rated current of the test object, while the measurement current only is $10\,\mathrm{A}$. Two different current sources are therefore needed. These are alternately connected to the test object, and are manually operated as a security measure against possible faults to prevent expensive devices to break. Another reason for this is the extra complexity it would add to the electrical solution, while removing only minor test operation work.

The warming device is an $18\,\mathrm{kW}$ heat exchanger. Oil is pumped out from the test tank into the heat exchanger and back again. It is here important to pump out oil from the bottom, since this is where the oil is coldest. Otherwise a huge temperature gradient will arise. The cooling device is a cold water copper pipe loop in the oil which is opened by a magnetic valve controlled directly from the computer relay. In this sense the cooling is not included in the safety solution, and this is of course due to the fact that it is only a good thing to cool the oil in the case of an emergency.

Finally, the measurement part of figure 10 consists of temperature and voltage measurements. Temperature probes are placed in six of the contacts, two of each material combination, and also at two places in the oil, near the bottom and top of the tank. These can be read automatically from the computer. The voltage drop over each contact is also measured, along with the voltage drop over a shunt put in series with the measurement current to get an accurate measure of its magnitude.

### 3.6.2  Software Solution

The electronic components were controlled by a LabView program. The program had four main components, a user interface, a control program, a measurement program and a power cycling program.

At the user interface, the user could supply the computer with the number of cycles, the duty cycle and the total time of the power cycle period. Here the user also supplied the cooling time for the thermal cycle. Finally, the user could tell the control program to launch or finish the measurement and thermal cycle period or power cycle period.

The control program took care of the temperature control relays, and launched the measurement and power cycling programs. When the measurement and thermal cycle period was started, the cooling was activated and the control program kept calling the measurement program as often as possible until the cooling time had elapsed. It then deactivated the cooling, activated the heating and returned to calling the measurement program as often as possible, until the user turned it off. It then stopped calling the measurement program and deactivated the heating. If the power cycle program was launched it sent the number of cycles, the duty cycle and the total time of the power cycle period to the power cycle program and waited for this to finish. When it had finished, generally after 14-18 hours, depending on when in the afternoon it could be started, it kept the heating and current on while waiting for the user to turn it off. It then deactivated the heating and current.

When called, the measurement program...

- activated the measurement current,

- waited for one second to allow current to stabilize,

- measured the voltages of the 15 contacts and the shunt by performing 10 measurement and saving the average,

- deactivated the measurement current,

- waited 5 seconds to eliminate the risk of interfering with the thermocouples,

- measured the temperatures, saved the time, temperature and voltages to a file and terminated.

When called, the power cycle program...

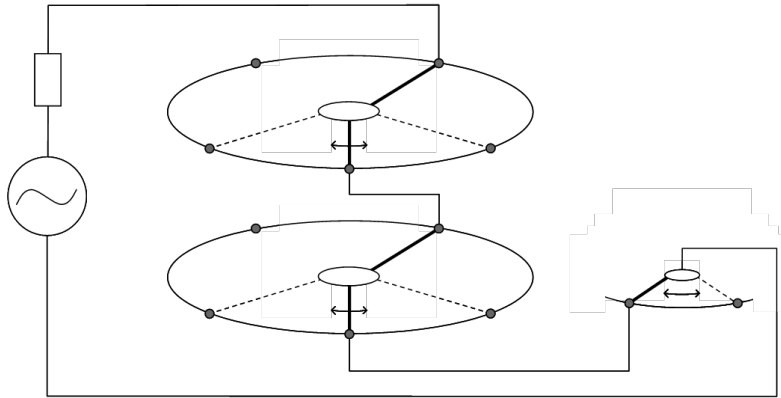- calculated the length of the power cycles and their frequency,

Figure 11: The test circuit for one phase of the tap selector. Two contacts are held fixed during the whole test and three contacts are operated once every week. The three phases are connected in series.

- activated the current and waited for the calculated cycle time, in the mean time measuring the temperature every 30 seconds,

- deactivated the current and waited for the next cycle to start, in the mean time measuring the temperature every 30 seconds,

- repeated the second and third steps until the start of the final cycle, when it only performed step 2 and then turned both heating and current off and terminated.

## 3.7   The Test Object

The test described above is performed on an ABB tap selector type I (see [26, p. 21]). Its rated current is 600 A divided on four contact fingers. The tap selector we use has six poles for the three phases. For each pole there exists five tap positions. A pre-selector, with two possible tap positions, is also available for each phase. The oil that will be used during the test is Nytro 10XN produced by Nynäs.

Using the setup shown in figure 11 five contacts can be tested in each phase. Two of these will be held static during the full test period, and will thus be a suitable reference with the AAFL test, as well as provide information of how the operation of the tap selector affects the contact resistances. The remaining three contacts will be operated at times corresponding to the maintenance intervals, which for tap selector type I is 7 years.

Three types of contact material combinations will be used. The purpose of performing the test with different materials is that the test method itself can

Table 3: Contact material combinations for the three phases, and the expected outcome of the experiment.

| Phase | Static contact | Sliding contact | Expected performance |
|---|---|---|---|
| 1 | Copper | Brass | Poor |
| 2 | Copper | Silver | Good |
| 3 | Silver | Silver | Excellent |

then be benchmarked against how the contacts are expected to perform in a life test of this kind. In this sense the test method itself is tested. The contact combinations to be tested are listed in table 3. To assure clean contact surfaces at the beginning of the test, all contacts were wiped with Scotch-Brite General Purpose Hand Pad. The contact pressures were measured and were all in the same interval as in commercial applications.

## 3.8   Evaluation Criteria of Test Results

To determine which contacts that pass the test, that is to be considered as long-term stable with respect to oxidation and coking, an evaluation of the data collected during the test period is made. The question is how evaluation criteria should be defined quantitatively to capture the properties of long-term stability in a realistic way, while still being intuitive and easy to calculate.

The parameter used in this test as a proxy of the "health" of the contact is resistance over the contact. To some extent it is acceptable that the resistance increases with time, but not to a too high level. The accepted increase can be measured in absolute or relative terms. To be as general criteria as possible to be able to cover a broad range of contacts a relative increase is chosen. A criterion based on an absolute increase is deemed to soon be outdated when development continues, and it will most likely not be backward compatible with products already on the market. The magnitude of the relative increase that is accepted is to be determined in the result section below, where the criterion is calibrated with the expected outcome of the test.

This criterion is similar to the first criterion of the AAFL test which states that a contact passes the test if the increase from the first to the 30th day is less than 25%. There are problems with this definition though, as was discussed in section 3.1. Some contacts naturally show a high initial resistance which then drastically decreases during the first few days. It is even possible to "dope" contacts to record a high initial resistance and thus

gain some extra margin to pass the test. This is not acceptable for a test method aiming to become a standardized test. We propose that the relative increase should be measured between the third day and the 30th day instead, to get around this problem. The idea is that the resistance measured the third day to a higher degree corresponds to the initial equilibrium resistance, than that of the first day. The first pass criterion is therefore:

$$\frac{R_{30}}{R_3} < c_1 \tag{11}$$

where $R_i$ denotes the mean resistance measured during day $i$. The constant $c_1$ is to be determined in the result section.

In addition to assuring that the relative increase in resistance not exceeds a certain level, it is also of importance for the long-term stability where this increase takes place. Imagine a contact which have a stable resistance for 25 days, which then suddenly starts to increase to a level right below the pass criterion in equation (11). A second criterion should be defined as to make this contact fail the test to keep it off the market since its long-term stability is highly questionable. This is also what the second criterion in the AAFL test sets out to do. It is formulated such that "stabilization should be reached" which leaves a rather arbitrary pass/fail decision in the hands of the test evaluator. To instead define a quantitative criterion to fail contacts where the resistance increase primarily takes place at the end we reason as follows.

All contacts experience some fluctuations in the resistance over the days. This is mostly due to the a-spot formations which take place during the load current period and varying characteristics of the surrounding of the contact spot. The strength of a good contact solution is that these fluctuations are quite small and, more importantly, that they do not increase too much with time. A contact solution that repeatedly fluctuates around its mean over the full test period should therefore pass the test. On the contrary, a contact solution that on the final day of the test repeatedly is on the high end of the measured values should fail the test. It is suitable to demand that the contacts should record a resistance below a 95% confidence interval around its mean resistance during the test period. In mathematical terms this can be defined as:

$$R_{30} < \mu + 1.96\sigma \tag{12}$$

where $R_i$ again denotes the resistance measured during day $i$, and $\mu$ and $\sigma$ is the mean and standard deviation, respectively, of the daily resistances over the test period.

It should be understood that the final resistance should turn out to be above this level in 5% of the cases if the trend in resistance is zero, and even

more often with a positive trend as is expected for most contact solutions. For a standardized test it is then a matter of defining how high ratio of contacts that are accepted to fail the second criterion defined in equation (12).

# 4   Silver Iodide and the Surface Structure of Silver Contacts

As discussed in 2.6, the black coating of the silver iodide disappears. This is not, as one could assume, due to the iodide being removed. In fact, approximately 80% of the iodide remains in the worn tracks of the contacts [19]. How the iodide can remain even though the contacts have left a distinct trace in the contact surface is not yet discovered. [27] describes a method for detecting pores in electroplated silver over bulk copper, the same substrate as many OLTC contacts. With that method pores as small as $2.5\,\mu$m (100 microinches) were detected. Guided by the theory that iodide could be accumulated in pores and scratches on the silver surfaces, briefly mentioned in [19] but not discussed or examined, we made a comparative study between wrought and plated silver, stationary and moving contacts, worn and unworn surfaces, silver iodide coated and pure silver surfaces. By doing so, we wish to get knowledge of what the different surfaces look like, and particularly study the presence of pores and scratches on the silver surfaces.

## 4.1   Initial Wear Process

Three contact combinations were selected for examination. They were installed into an OLTC and dried off with ethanol drenched paper towels. The OLTC was then operated 400 times. The contacts were mounted in the change-over selector of an ABB tap selector size III to create as true a replica of their working kondition as possible. This is not an exact replication of their true environment though, since they were not operated in transformer oil, and temperature was approximately $22\,^\circ$C, far lower than the regular temperatures OLTCs operate in. There were two sorts of fixed contacts available: $(i)$ electroplated silver on bulk copper contact, from here on denoted Ag(p), and $(ii)$ the same contact, but coated in silver iodide, from here on denoted AgI(p). For the sliding contacts, there were also two options: $(i)$ wrought silver, from here on denoted Ag(s)[7] and $(ii)$ electroplated silver on bulk wrought silver, from here on denoted Ag(p). The evaluated contact combinations can be seen in table 4.

The fixed contacts of the three combinations all had to be mounted at the same time. They were covered in cardboard to protect them from metallic dust falling down on them when wearing the contacts above. Since the contacts were going to be examined in a SEM, dust falling on the contact area after the wear process seemed even more harmful than dust falling before the

---

[7]Wrought in Swedish is "smidd", thus the "s".

39

Table 4: Evaluated contact combinations in the SEM analysis.

| Fixed contact | Moving contact |
|:---:|:---:|
| Ag (p) | Ag (s) |
| Ag (p) | Ag (p) |
| AgI (p) | Ag (s) |

wear. The wear process where thus performed on the top contacts first and then moving down.

The tap changer was maneuvered with a drilling machine with the same speed as the tool that operates the tap changer in the field. One should be aware though, that the drilling machine lost much speed and force during the experiment as a result of both heating and low battery.

After the tap changer had been operated 400 times with each contact combination, the contact areas were covered with paper towels. The contacts were cut as close as possible to the contact area without harming it to better fit in the SEM. They were then wrapped in more paper and transported to Gothenburg in a bag for SEM analysis.

## 4.2 Scanning Electron Microscope Analysis

Before being placed in the SEM, the contacts were washed with ethanol and then blow dried using compressed air. They were then inserted in the SEM from which the air was pumped to create a vacuum.

During the microscopy, we consequently used 15 kV EHT and almost always 10 μm aperture. 30 μm aperture was used at a few occasions but tended to burn the surface with too much electrons and was thus abandoned. We began by taking a picture of the worn tracks with a small magnification of 100 using SE2 and working distance 10 μm and then zoomed in as far as possible while still attaining a focused image, generally to magnifications of around 10-15 000 times. We then zoomed out and changed to InLens and once again zoomed in as far as possible while still attaining a focused image, generally reaching magnifications of around 30-60 000 times. With the InLens we used both 10 μm and 3 μm working distances. The EsB detector was then chosen and both topographic and atomary measurements, primarily using working distance[8] 3 μm but occasionally 10 μm. Finally, we returned to 10 μm and switched to EDX analysis and analysed the material composition.

---

[8]The working distance of the microscope is the distance between the bottom of the objective lense and the specimen [20, p.143].

The procedure was repeated for the areas outside the worn track for reference. Due to time shortage only the first three contact combinations were examined.

# 5    Results

## 5.1    Oxidation Endurance Test

In the following the results of the oxidation endurance test will be presented. First the contact resistance data will be presented and second the temperature data collected during the test. Throughout this section the contact materials will be referred to as Cu/Brass, Cu/Ag and Ag/Ag, where Cu, Br and Ag stands for copper, brass and silver, respectively. The meaning of Cu/Brass is further that Cu is the static contact material and Brass is the sliding contact material. The measurement current is 10 A for all resistance results shown below.

In figure 12 a main result of the thesis is presented. The development of contact resistance as a function of the number of days passed since the test started is shown. Each point is a mean over the five contacts of each contact material (in the beginning of the test) and a mean over the collected data each day, resulting in three data points per day. In the figure one can see that the material combination expected to perform poorly indeed does so. The resistance increases rather constantly over the course of the test period. In the figure special events are also noted with arrows. After just a few days a test breakdown occurred due to a meltdown of a contactor delivering current to the oil heat exchanger. Unfortunately, this took place on the second day of a four day holiday, so that the test stood for three days. On the following week-day the contactor was replaced so that the test could be continued. More on this later.

The scheduled operation times can also be noted in the data of figure 12. These were performed each 7th day of aging, corresponding to the maintenance interval of 7 years of the test object. An increase of contact resistance can be noted the first operation for all contacts, but a decrease can be seen for Cu/Brass the second operation. In table 5 this can be seen more clearly. Here before and after resistance data is given, and it can be seen that change in resistance can be both positive and negative, although it is more frequent that the resistance increases after an operation. An exception of this is when the resistance initially is high, then it tends to decrease at operation. This is expected, and is called the "wiping effect". An oxidized contact can be temporarily cleaned this way. It should be emphasized, though, that one cannot draw any far fetched conclusions from the data given in 5. To do this a greater volume of data is needed to get some statistics.

Finally, it can also be seen in figure 12 that two Cu/Brass contacts were removed due to runaway behavior. After this the mean resistance for this materail combination decreased instantly but the rate of change was still

Table 5: Contact resistance before and after the first two operations. The contact types represent I) operated contact in fine selector, II) operated contact in pre-selector, III) contact not operated in fine selector. The material combinations are given as static/sliding contact. The difference in resistance can be both positive and negative.

| Contact type | Material | Resistance [$\mu\Omega$] | | | | | |
|---|---|---|---|---|---|---|---|
| | | B. op1 | A. op1 | Diff op1 | B. op2 | A. op2 | Diff op2 |
| I | Cu/Brass | 181 | 189 | +8.0 | 806 | 569 | -237 |
| I | Cu/Brass | 33.6 | 208 | +175 | 317 | 49.7 | -268 |
| I | Cu/Ag | 10.5 | 148 | +137 | 82.0 | 341 | +333 |
| I | Cu/Ag | 10.9 | 234 | +223 | 23.0 | 521 | +498 |
| I | Ag/Ag | 7.2 | 15.4 | +8.1 | 5.2 | 13.2 | +8.0 |
| I | Ag/Ag | 6.2 | 12.7 | +6.5 | 6.9 | 6.4 | -0.5 |
| II | Cu/Brass | 195 | 135 | -59.9 | 658 | 57.1 | -601 |
| II | Cu/Ag | 17.8 | 160 | +142.6 | 28.2 | 230 | +202 |
| II | Ag/Ag | 3.8 | 11.5 | +7.8 | 3.8 | 17.3 | +13.5 |
| III | Cu/Brass | 106 | 175 | +68.5 | 195 | 305 | +110 |
| III | Cu/Brass | 92.6 | 360 | +267.8 | 1 083 | 1 311 | +227 |
| III | Cu/Ag | 18.2 | 16.2 | -2.0 | 12.6 | 18.4 | +5.8 |
| III | Cu/Ag | 11.7 | 14.6 | +2.9 | 20.2 | 28.7 | +8.5 |
| III | Ag/Ag | 8.5 | 7.7 | -0.8 | 5.4 | 5.9 | +0.5 |
| III | Ag/Ag | 4.7 | 7.8 | +3.1 | 2.8 | 3.7 | +0.9 |
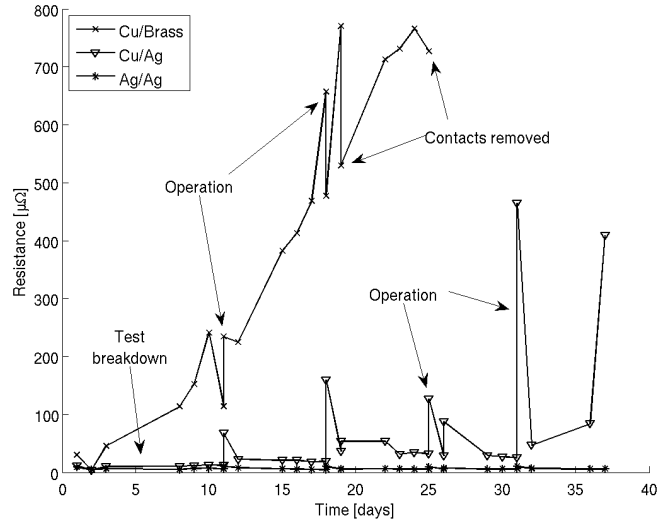
Figure 12: Mean contact resistance of the three contact materials each day, though no data was collected during weekends. Special interference with the test is noted with arrows. A magnified version of this figure regarding Cu/Ag and Ag/Ag can be seen in figure 13.

positive.

Figure 13 shows two zoomed in versions of figure 12, focusing on the Cu/Ag and Ag/Ag contact materials which have a much lower resistance compared with Cu/Brass. It is noticeable that the resistance is rather constant in between the events of the test. Both material combinations experience resistance increase when operated, and both regain the low resistance level to some extent. This can most likely be dedicated to the large load current during the night time aging, which "burns" through the temporarily formed oxide layer between the contacts, so that a good contact is reestablished. This is a well known effect called fritting. It is the case though, especially for Cu/Ag, that a non-negligible shift takes place in the upward direction at each operation.

In figure 14 a mean of each contact material at each measurement time is given. The figure is quite cluttered, but should give an insight about that the resistance is non-constant during the span of a day. This is the underlying data of figure 12 and 13 discussed above. The gaps between the data deserve its own mentioning. First, one can see that the resistance measurements only are performed during the oil temperature cycle each day, when the load current is off. This is the case since the voltage measurement device used is disturbed heavily when the load current is on, and thus delivers unreliable

44

(a) Cu/Ag and Ag/Ag                    (b) Ag/Ag
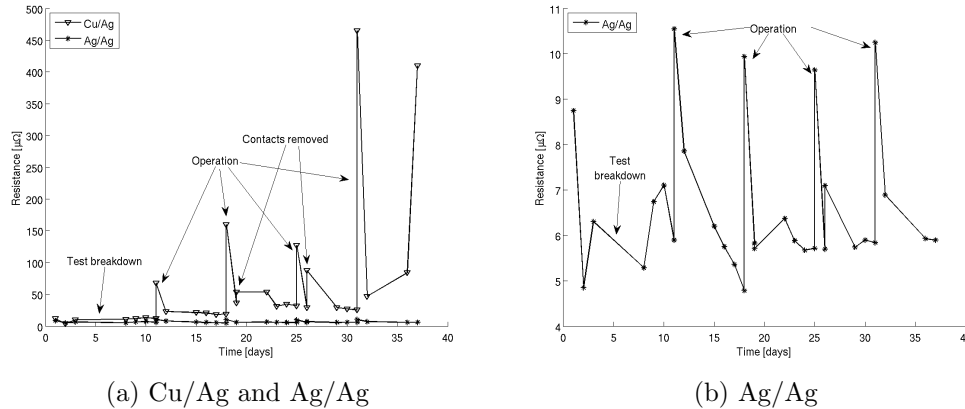
Figure 13: Mean contact resistance of the two contact material combinations Cu/Ag and Ag/Ag in (a) and a zoom in on Ag/Ag only in (b). Special interference with the test is noted with arrows. A version of this figure with Cu/Brass included can be seen in figure 12.

data. Second, one can notice the week-ends, during which the manual operation of connecting the measurement current cannot be performed. The test is automatically run in the same fashion as during the week-days, only that no data can be collected. Third, the test breakdown mentioned above took place during day 4-6. The gap in the data would actually have been there in any case due to the holiday, but the aging of the test object is postponed for three days.

The development of the individual contacts can be seen in appendix B. Most notably is that the individual contacts differ quite much in their performance, even within the same material family. It is not the case that the "resistance ranking" between the contacts is fixed, but instead the contacts perform good and bad during different periods of time. This can be attributed to the cycling of both oil temperature and load current, which adds a stochastic element to the performance of the contacts since it sometimes hits a good contact spot during the induced thermal deformations, and sometimes not.

During day 19, as can be seen in figure 12, two Cu/Brass contacts were bypassed and removed from the test due to their too large resistance. The remaining three Cu/Brass contacts were finally removed day 25. To keep them in the test was not an option, since they would jeopardize the stability of the load current and also deteriorate the quality of the oil. At a load current of $1200\,\text{A}$ and a contact resistance of over $1\,\text{m}\Omega$ a point source of

45
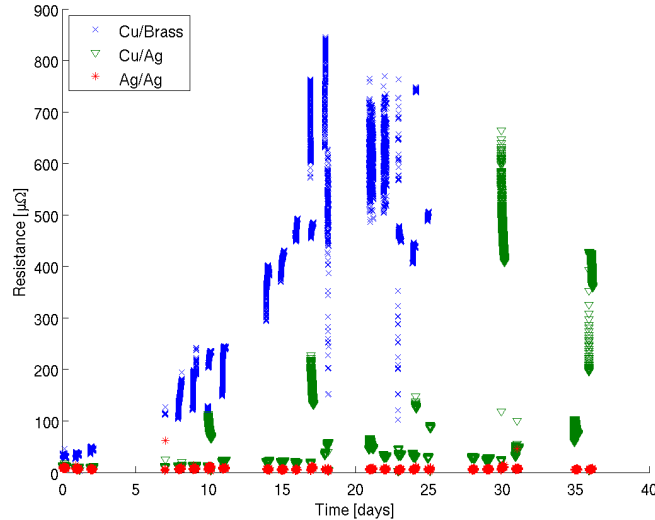
Figure 14: Mean contact resistance of the three contact materials for all measurement times. The reoccurring gaps in the data corresponds to weekends, and data was thus not collected here, although the test object was still aging at these times. A test breakdown occurred during days 4-6.

heat of $1\,\mathrm{kW}$ is realized. This induces chemical reactions in the oil and the risk of fire and circuit break, both of which are not desirable.

The removal process itself consisted of cooling the oil to about $60\,^\circ\mathrm{C}$ whereafter it was pumped out of the tank. The wires could then be changed as to bypass the failed contacts. The oil was then pumped back into the tank and the test was continued. The whole process took approximately 4 hours and was neglected in terms of lost aging time.

Figure 15 shows the individual raw data of each contact for a period of three days. Here, again, one can notice the largely varying behavior of the Cu/Brass contacts, especially during day 9. The resistance varies both in the positive and negative direction, mostly due to the cooling and warming of the oil. The figures for Cu/Ag and Ag/Ag can be hard to interpret in a black and white print, but the essence is that these contacts lie quite constant over time, although with a rather large standard deviation of the measurement data.

Moving on to temperature data, the oil temperature over the test period can be seen in figure 16. In 16a the temperature at the surface of the oil is shown, while the temperature at the bottom is shown in 16b. During the commissioning of the test large temperature gradients were noticed, but an extra oil pump was installed to get a better circulation of oil from the warm

(a) Ag/Ag

(b) Cu/Ag
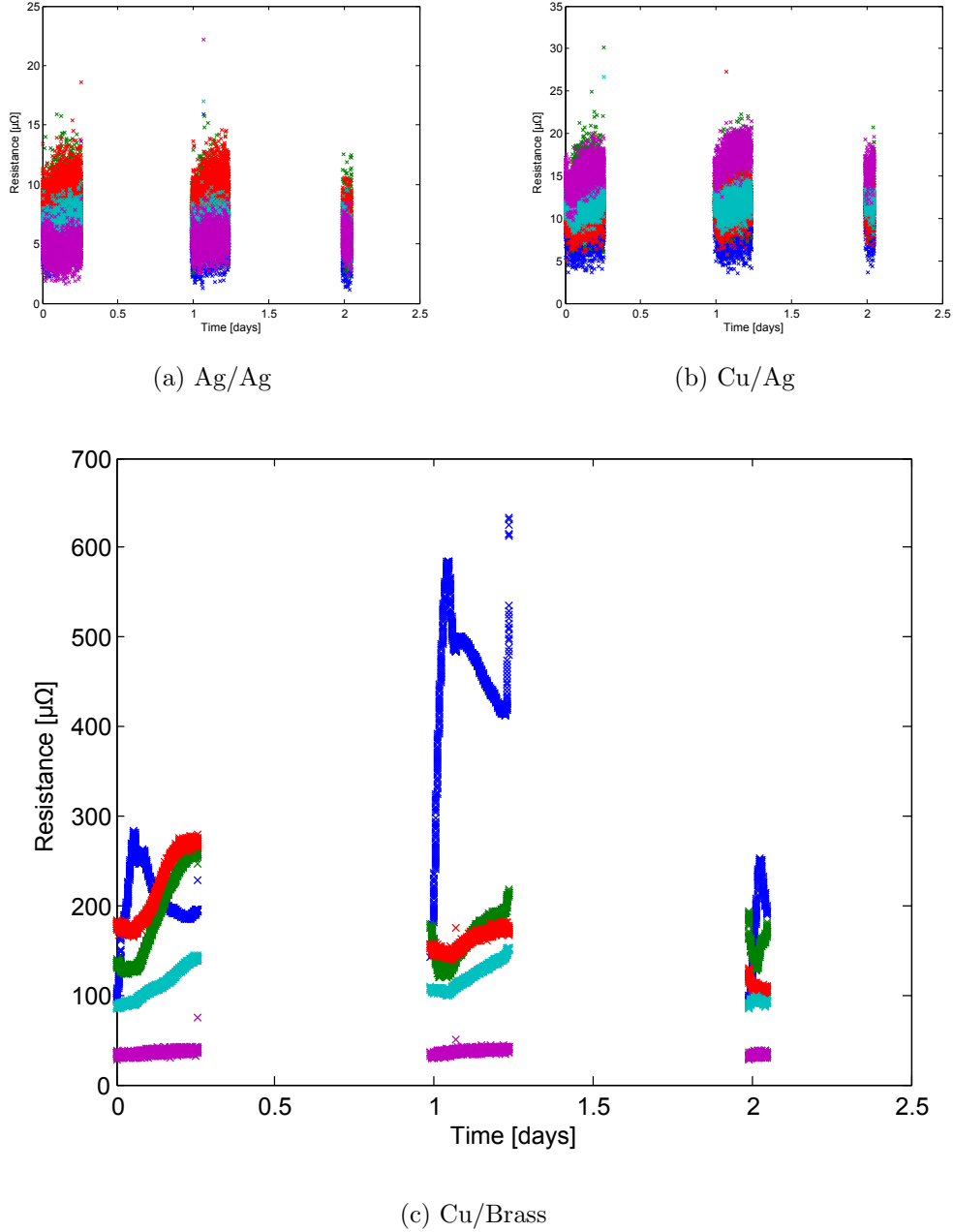
(c) Cu/Brass

Figure 15: Individual contact resistance measurements during the days 8-10 (In color). Notice the largely varying behavior of the Cu/Brass contacts, especially during day 9. The resistance varies both in the positive and negative direction, mostly due to the cooling and warming of the oil. The figures for Cu/Ag and Ag/Ag can be hard to interpret in a black and white print, but the essence is that these contacts lie quite constant over time, although with a rather large standard deviation of the measurement data.

surface to the cold bottom. Still, slight temperature differences of a few degrees Celsius can be noted, but these are tolerable.

The lowest temperature during the oil temperature cycles can be read out of the figures to be 60 - 70 °C, which is a good result regarding the goal of 50 °C temperature cycles over the day. It is also good to notice that the plateau at maximum oil temperature is at right above 120 °C, which was the target of the test. The disturbance of the data, with the "thick" lines at the maximum plateau and the jumping back and forth between reasonable numbers and 20 °C (set to be the lowest possible), is hard to explain. It might be due to disturbance from the load current, or the equipment is not stable enough.

During the days 19-21 there is a shift downwards in figure 16b compared with earlier data in the series. This is due to that the sensor was lowered a bit further in the oil tank during the removal of the Cu/Brass contacts discussed above. The lowest located contact is higher up in the tank than this, though, approximately on the level it was placed before, so that the temperature gradient is tolerable. Still, it is interesting to see how quickly the oil temperature decreases when the sensor is lowered only a few centimeters.

In figure 17, the last temperature figure, the temperature variation of the contact bulk during two different days are presented for one contact of each material combination. As have been previously described, the load current is cycled to put thermal stress on the contact spots. During the first day, the contacts all have temperature increments over the oil temperature in the interval 10 to 30 °C. A few days later, on day 20, these numbers have changed to 10 to 130 °C, a remarkable increase in spread. In table 6 this spread is quantified, and the temperatures immediately after the load current is turned of are shown together with the thermal equilibrium which is reached after a few minutes and coincides with the oil temperature.

In both the figure and the table it is seen that the Cu/Brass contact has a much higher temperature after 20 days (250 °C) compared with the first day (150 °C). This is expected, since the increased resistance generates more heat in the contact spot due to $P = RI^2$. An increase can be seen also for Cu/Ag (increase from 140 °C to 170 °C), but for Ag/Ag it is hardly noticeable.

The temperature measurement might be disturbed when the load current is applied and is not completely reliable, although it often shows plausible values. An exception to this is the values for Ag/Ag shown in figure 17b, where the temperature under load is registered as lower than the oil temperature. This is certainly not a credible result. Immediately after the load current is turned off, though, expected values are again given and it also follows the shape of the Cu/Brass and Cu/Ag curves closely.
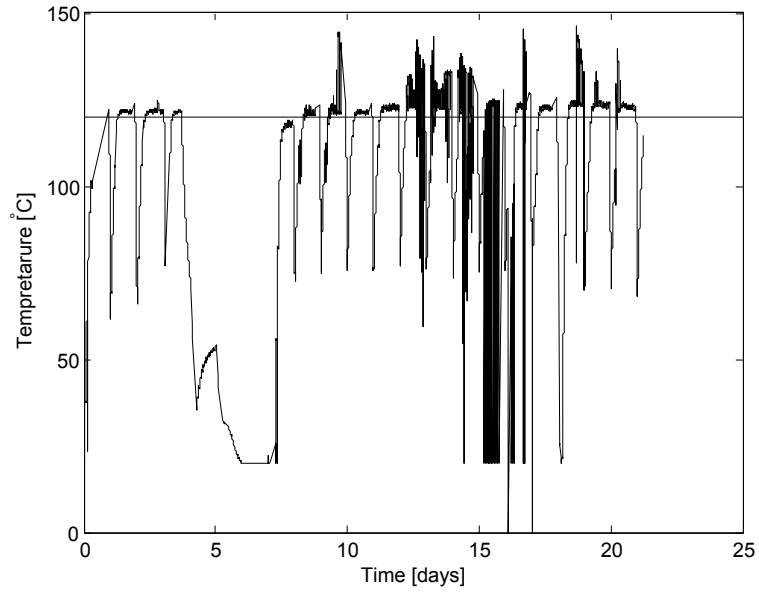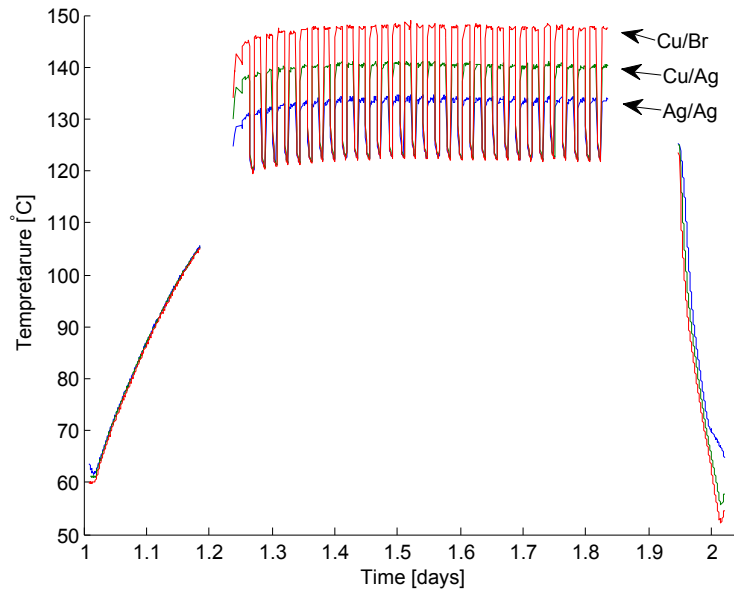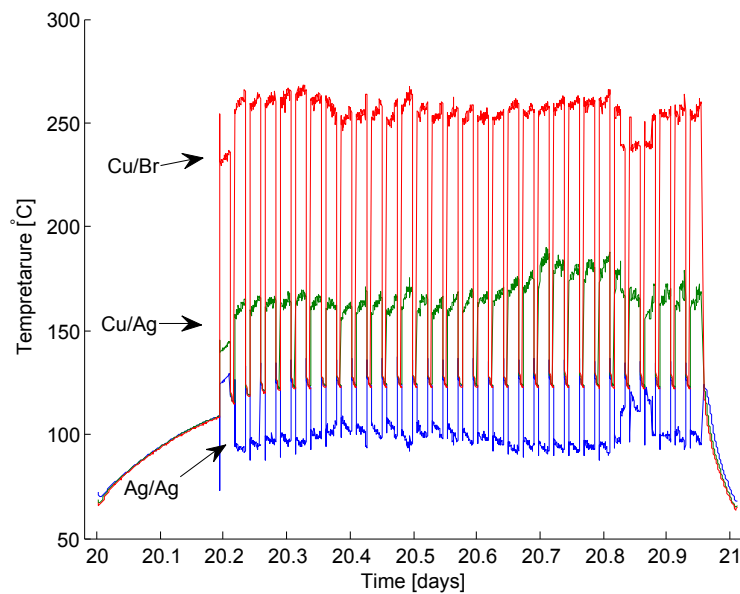
(a) At surface.
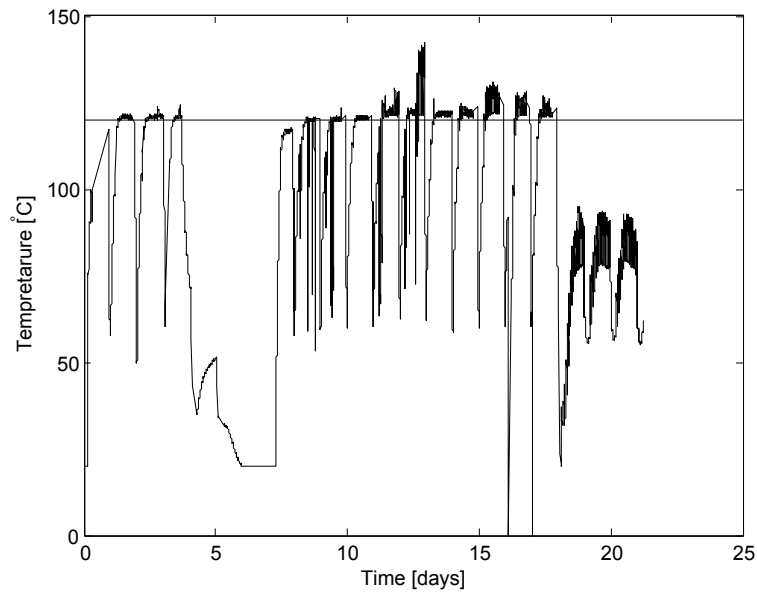


(b) At bottom.

Figure 16: Temperature of the oil during full test period. The test breakdown during days 4-6 can be seen. The low sensor in (b) was moved further down at day 18. The plateau at maximum oil temperature is at right above 120 °C, which was the target of the test.

(a) Day 1



(b) Day 20

Figure 17: Temperature of the contact bulk over day 1 and day 20 for one contact of each material combination.The temperature measurement might be disturbed when the load current is applied and is not completely reliable, although it often shows plausible values. An exception to this is the values for Ag/Ag shown in the bottom figure, where the temperature under load is registered as lower than the oil temperature, which is certainly not a credible result.

Table 6: Contact bulk temperature of sliding contact immediately after current cycle as well as thermal equilibrium without load current for one contact of each material combination during day 1 and 20. The material combinations are given as static/sliding contact.

| | Temperature [°C] | |
| --- | --- | --- |
| Contact material | Day 1 | Day 2 |
| Cu/Brass | 147.5 | 255.2 |
| Cu/Ag | 140.3 | 164.8 |
| Ag/Ag | 133.7 | 134.7 |
| Th. eq. | 122.0 | 122.3 |

Table 7: Oxygen concentration in the oil prior to, during and after the test in parts per million by volume. The numbers in parenthesises refers to days from or before the commencement of the test, the other numbers refers to days of aging. This is due to the test breakdown in the first week.

| Day | Oxygen concentration [ppm] |
| --- | --- |
| (-5) | 12 000 |
| 0 (0) | 25 000 |
| 7 (10) | 24 000 |
| 14 (17) | 21 000 |
| 21 (24) | 22 000 |
| 27 (30) | 22 000 |
| 33 (36) | 25 000 |

### 5.1.1   Oxygen concentration

The oxygen concentration was measured each time the tap selector was operated. Initially the concentration was low, only 12 000 ppm by volume, but the oil was left in the open container for 5 days in ambient temperature and with no current running.When the test was started, oxygen levels had risen to 25 000 ppm and remained between 21 000 and 25 000 ppm for the remainder of the test. The measured oxygen concentrations can be seen in table 7.

### 5.1.2   Application of the Test Criteria

Here the criteria described in section 3.8 above will be calibrated against the outcome of the test. Since the test is thought to be carried out successfully, so that a calibration of this kind is possible, the expected performance of the different contact solutions (listed in table 3) will be reflected in the contact's result in the test.

With the constant $c_1$ in equation (11) equal to 3 a good calibration is reached. In the figures 18 and 19 the result of the individual contacts is shown graphically for the Cu/Ag and Ag/Ag contact solutions, respectively. The Cu/Brass contacts are of course all judged to fail the test since they were taken out of the test prematurely. For convenience, the criteria from section 3.8 are again given here:

$$\frac{R_{30}}{R_3} < 3$$

$$R_{30} < \mu + 1.96\sigma$$

Expressed in words the criteria say that the contact resistance cannot increase more than 200% from day 3 to day 30, and that the resistance on day 30 is below a 95% confidence interval above the mean resistance over the test period.

In the figures 18 and 19 the upward sloping red line corresponds to the first pass criterion and the horizontal red line corresponds to the second criterion. For a contact to pass the test the resistance at day 30 should be below both of these red lines. The dashed red line represents the first criterion in the AAFL test, for comparison. It should be noted that the test performed here is a tougher test for the contacts, though, and that it therefore is not directly applicable.

With these two criteria we can read out from the figures 18 and 19 that 2 out of 5 of the Cu/Ag contacts pass the test (with 2 just failing on the first criterion) and that all 5 Ag/Ag contacts pass the test with distinction.
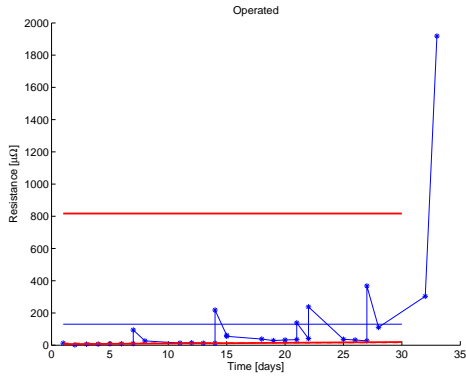
(a) 06, Cu/Ag
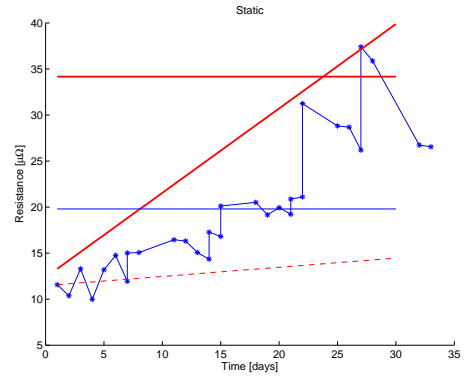
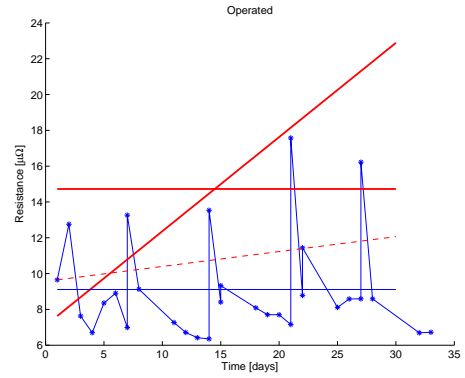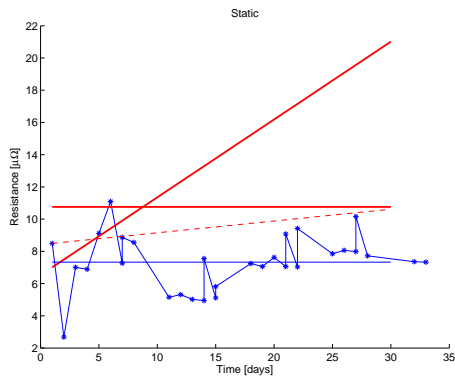(b) 07, Cu/Ag
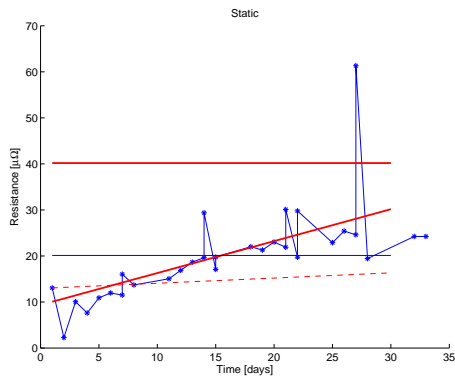
(c) 08, Cu/Ag
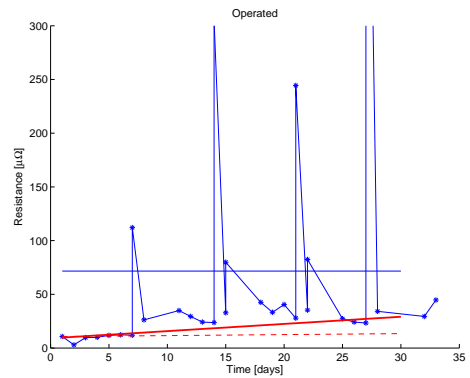
(d) 09, Cu/Ag
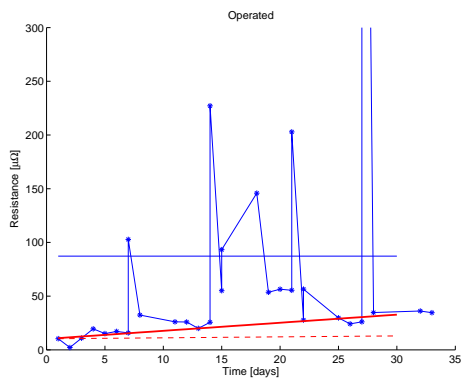
(e) 10, Cu/Ag

Figure 18: Test results of individual Cu/Ag contacts when the test criteria have been applied. The resistance at day 30 should be below both the two red lines for the contact to be considered passed. The contacts in (c) and (e) have passed the test, the others have failed.
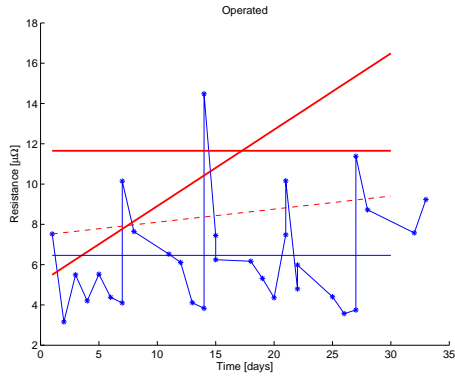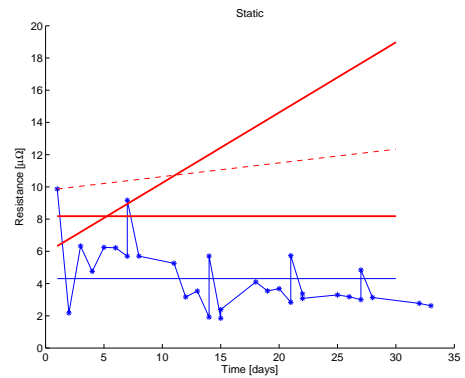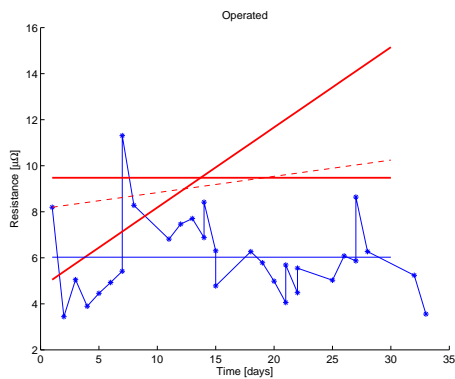
(a) 11, Ag/Ag

(b) 12, Ag/Ag

(c) 13, Ag/Ag

(d) 14, Ag/Ag

(e) 15, Ag/Ag

Figure 19: Test results of individual Ag/Ag contacts when the test criteria have been applied. The resistance at day 30 should be below both the two red lines for the contact to be considered passed. All Ag/Ag contacts easily passed the test with the suggested criteria.

54

## 5.2   Silver Iodide and the Surface Structure of Silver Contacts

Here we present the most illustrative of the SEM pictures taken on the various contacts. Figure 20 shows the unworn surface of a fixed Ag(p) contact. It has clearly visible pores in the surface, about 200 nm wide. It also has some smaller structures which might be pores, though magnification and resolution are not great enough to say clearly.

Figure 21 shows a worn track on the surface of a fixed Ag(p) contact. Also here there are pores present, even though the surface has been passed by a moving contact 800 times (back and forth for 400 operations).

In figure 22, the worn track of a fixed Ag(p) contact is studied at another location. It shows a distinct crevice in the surface. There are no clearly visible pores, even though the surface, in an out of the crevice, show some slight surface roughness.

Figure 23 shows the unworn surface of a moving Ag(s) contact. Also this surface has crevices, but no sign of the small pores in figures 20 and 21. The surface structure is very different from the fixed Ag(p) with much larger structures.

In figure 24 the worn tracks of a moving Ag(p) are displayed. Once again, the crevices are present. The surface structure is a hybrid of the moving Ag(s) and the fixed Ag(p) with the large structures of the Ag(s), but a surface roughness that resembles the fixed Ag(p). No sign of pores on this surface, though.

Figure 25 shows the unworn surface of a moving Ag(p) contact. Its surface structure does not resemble the fixed Ag(p). On a coarser scale, the structure of the Ag(s), which the electroplated silver has been applied on, can be seen, see figure 25a. At greater magnification though, it has its own distinct structure, with lots of surface roughness, see figure 25c.
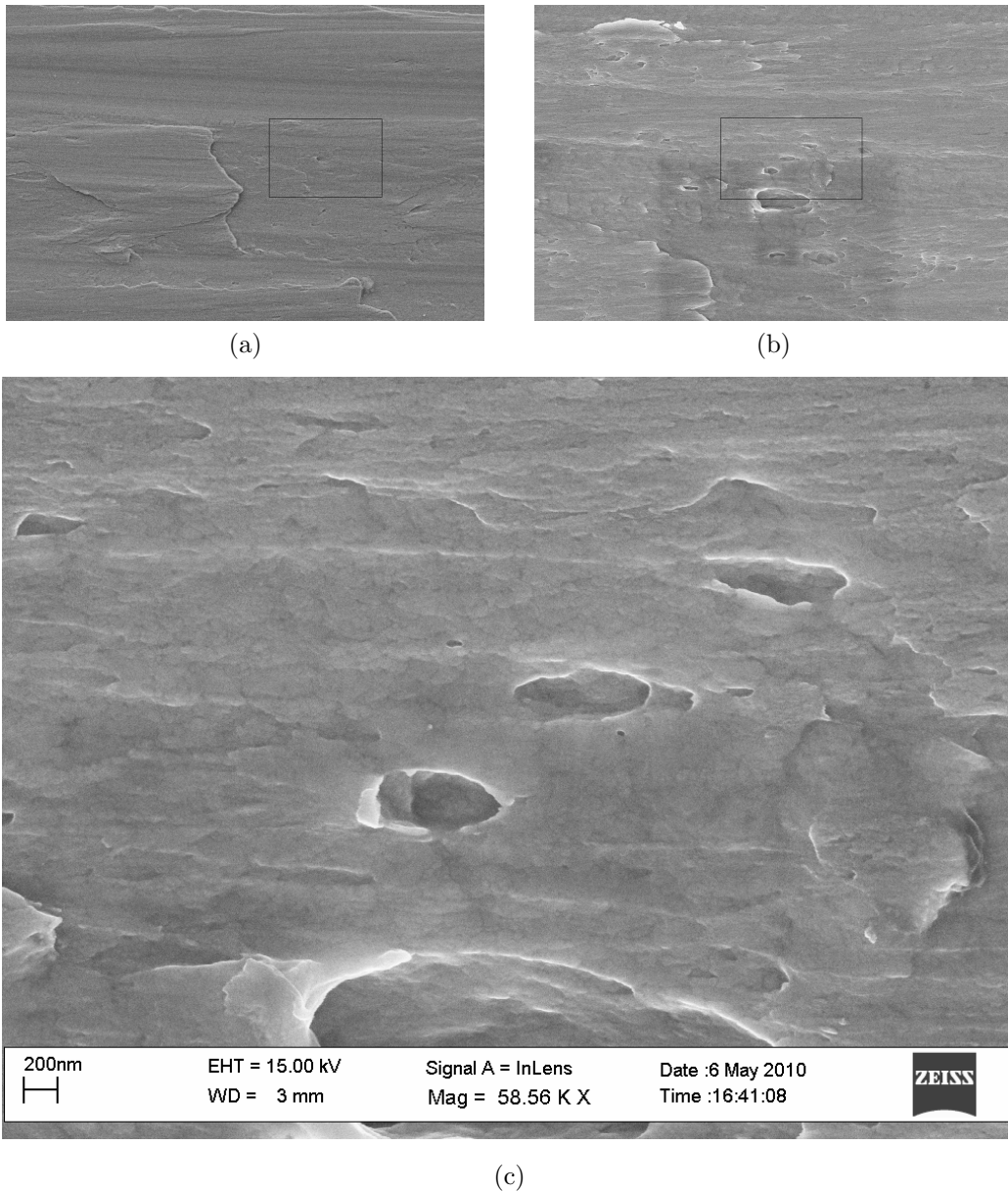
(a)                                           (b)



| 200nm | EHT = 15.00 kV | Signal A = InLens | Date :6 May 2010 | ZEISS |
| | WD =   3 mm | Mag =  58.56 K X | Time :16:41:08 | |

(c)

Figure 20: The unworn surface of a fixed Ag(p) contact. Clearly visible pores are present on the surface, about 200 nm wide.

56

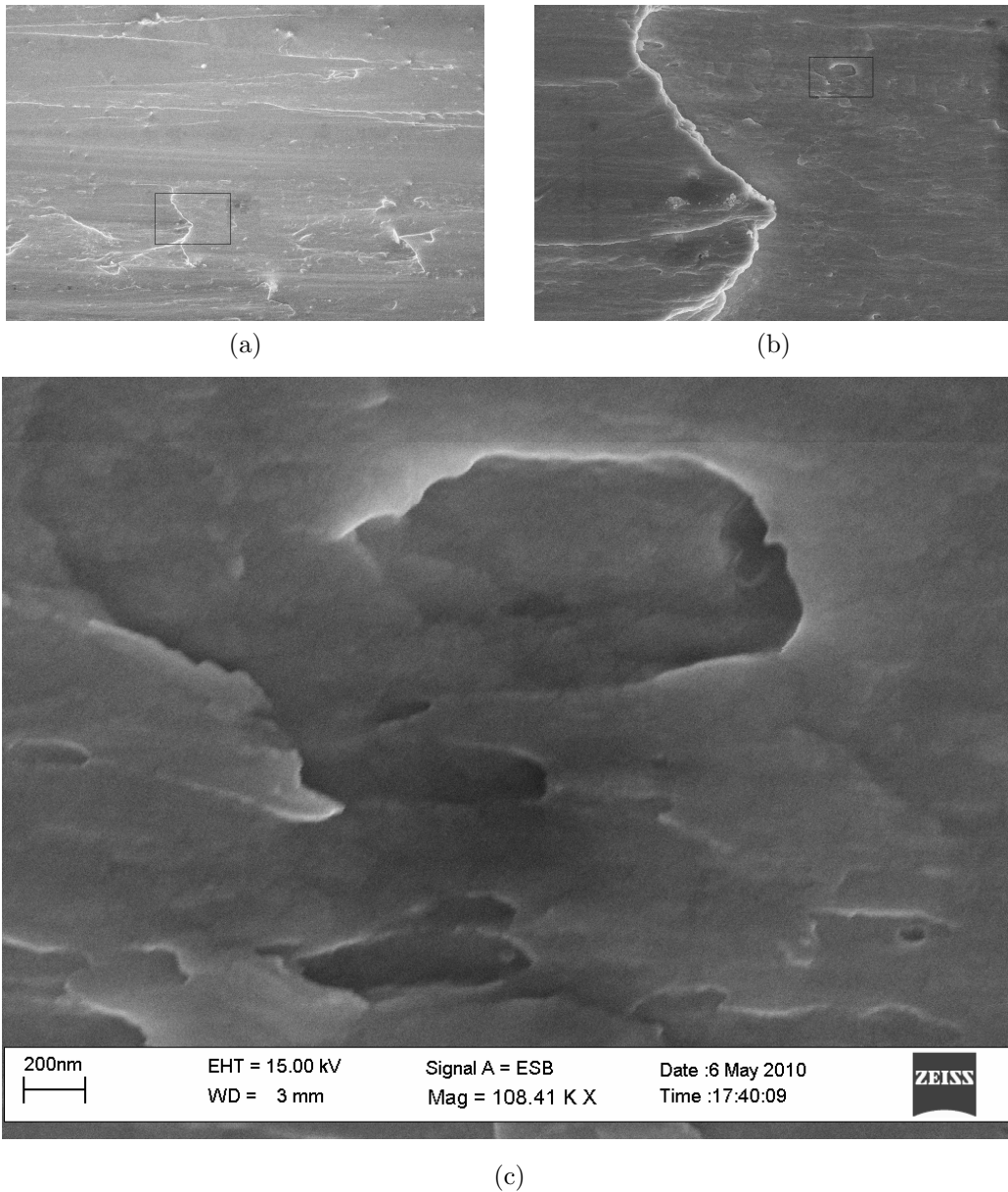(a)                                          (b)

(c)

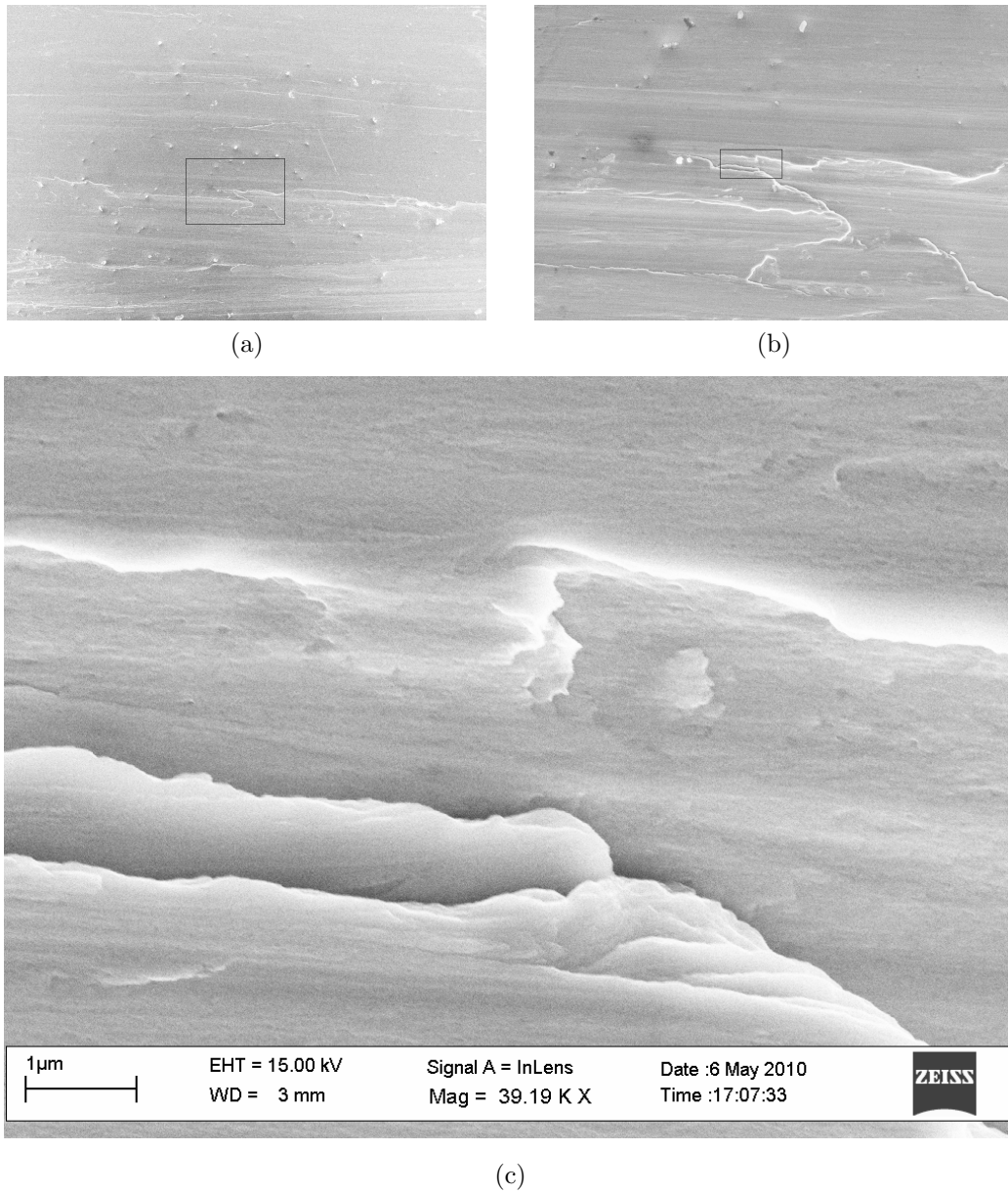Figure 21: Pores in the worn tracks of a fixed Ag(p) contact. The surface has been passed by a moving contact 800 times.

(a)



(b)



| 1µm | EHT = 15.00 kV | Signal A = InLens | Date :6 May 2010 | ZEISS |
| | WD =   3 mm | Mag =  39.19 K X | Time :17:07:33 | |

(c)

Figure 22: Crevice in the worn tracks of a fixed Ag(p) contact. No pores are visible, just slight surface roughness.

58

(a)

(b)

(c)
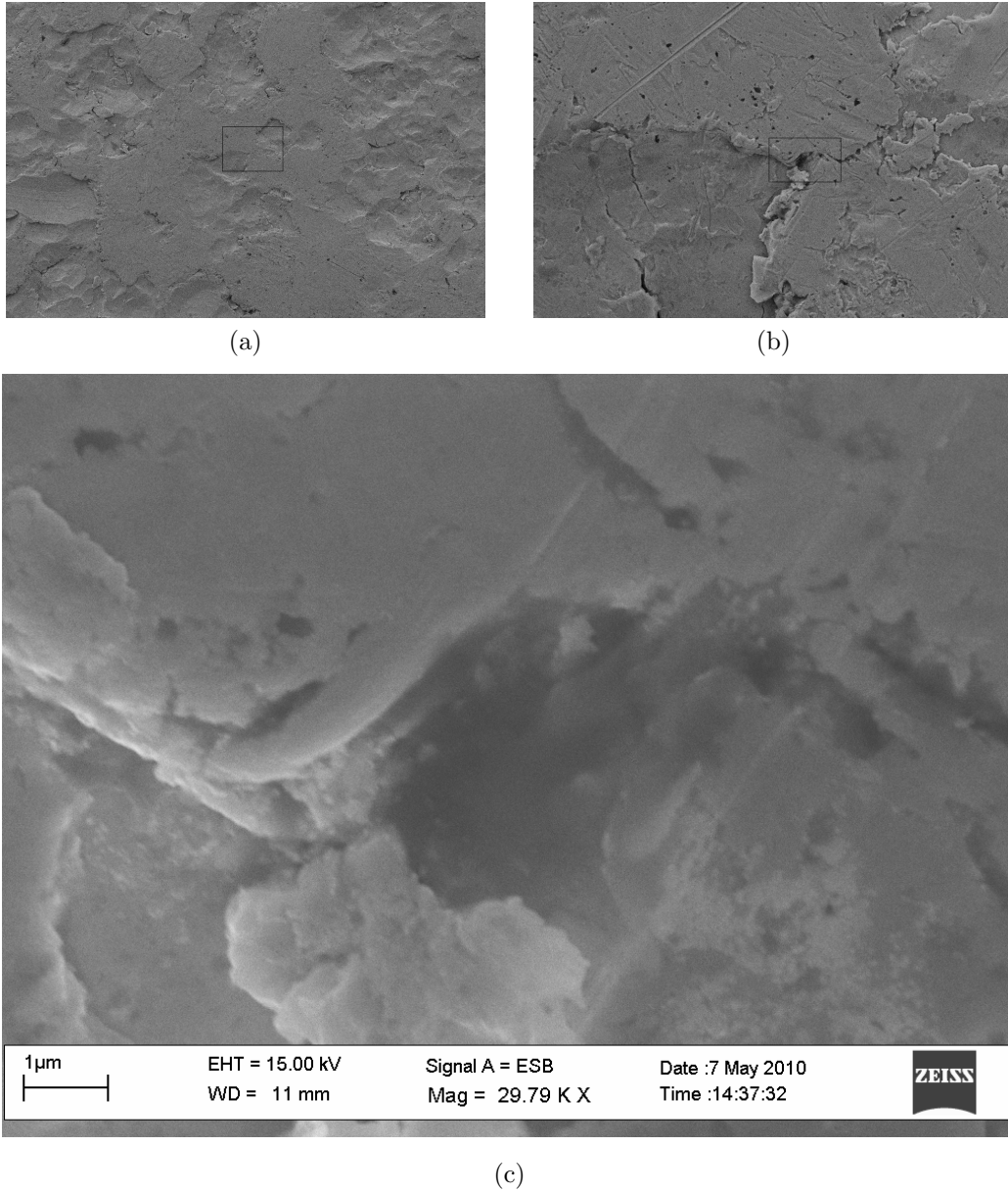
Figure 23: Crevice on an unworn moving Ag(s) contact. The surface structure is very different from the fixed Ag(p) with much larger structures.

59

(a)


(b)



| 20µm | EHT = 15.00 kV | Signal A = SE2 | Date :6 May 2010 | ZEISS |
| | WD =  9 mm | Mag =  1.10 K X | Time :18:48:40 | |

(c)
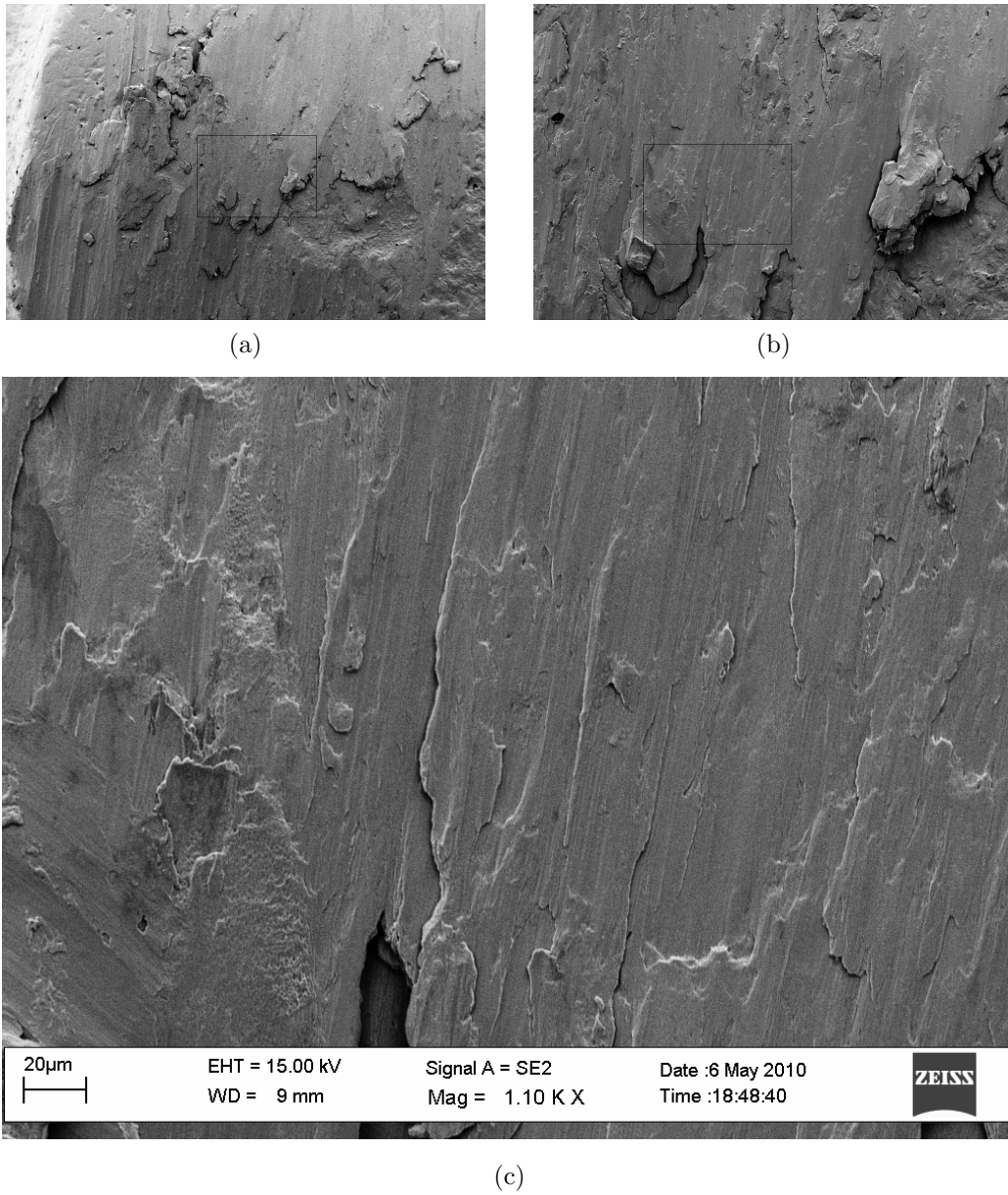
Figure 24: Crevices in the worn tracks of a moving Ag(p) contact. The surface structure is a hybrid of the moving Ag(s) and the fixed Ag(p) with the large structures of the Ag(s), but a surface roughness that resembles the fixed Ag(p) but with no sign of pores.

(a)                                                     (b)



(c)
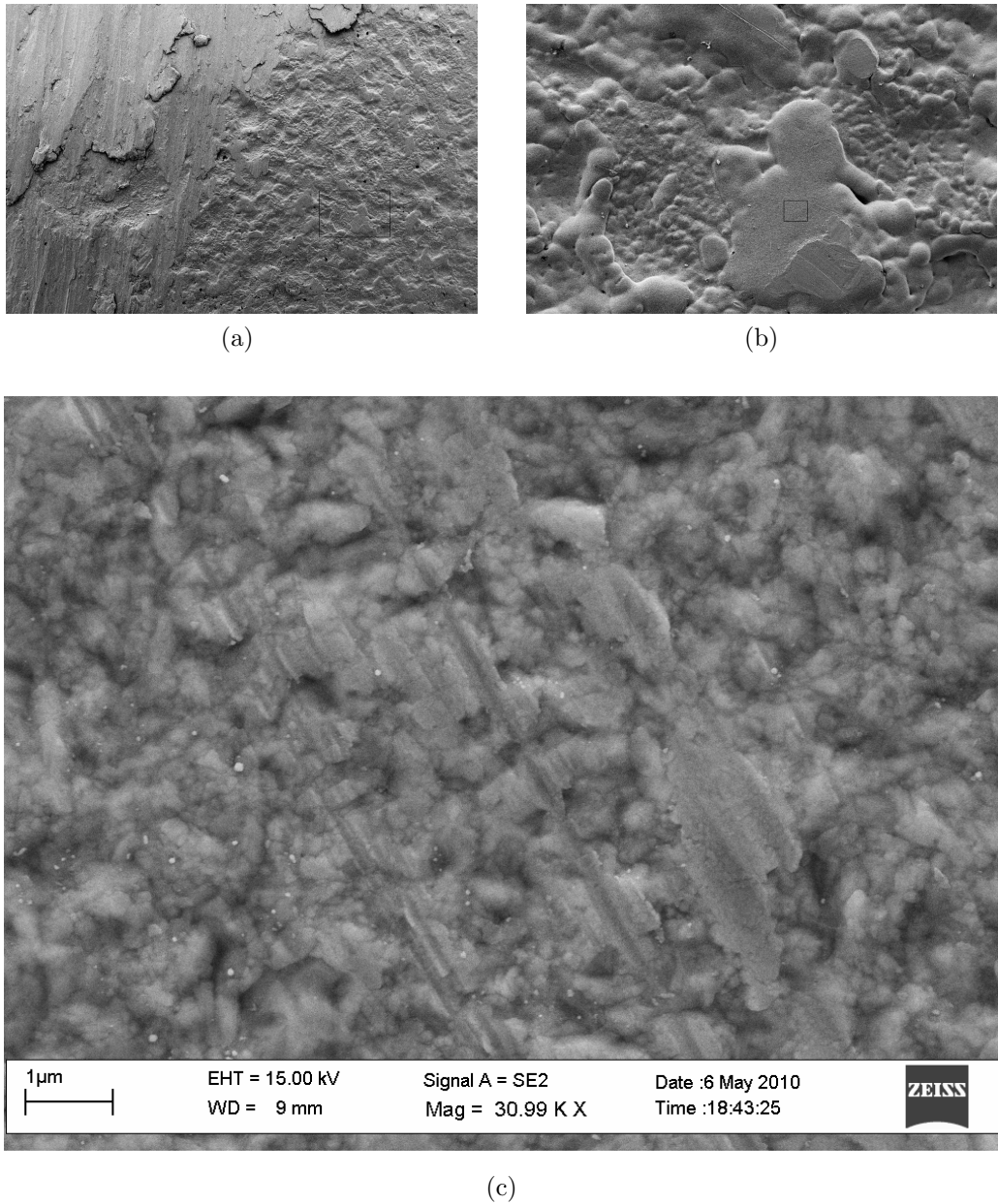
Figure 25: Surface structure of unworn moving Ag(p) contact. Its surface structure does not resemble the fixed Ag(p). On a coarser scale, the structure of the Ag(s), which the electroplated silver has been applied on, can be seen, but at greater magnification it has its own distinct structure, with lots of surface roughness.

# 6    Discussion

In this section, the results of the thesis will be discussed and analyzed from a broader perspective. Assumptions discussed earlier will be checked when possible and improvements of the implementation of the tests will be suggested.

As the thesis have been structured above, the oxidation endurance test will first be discussed, followed by a discussion of the surface structure of contacts.

## 6.1    Oxidation Endurance Test

To perform an accelerated life test that reflects the behavior of real life operation is indeed a challenging task. It can be precarious to draw too far fetched conclusion from the result as they might not mimic reality close enough. On the other hand, one often needs to consult accelerated life tests to at least get some indication of how a product may perform during a long lifetime, because otherwise there would be no experimental guidance at all. And this is of course the strength of the approach.

When it comes to the acceleration of product aging regarding OLTCs there is already a rather good proposal available, above called the AAFL test. A norm committee is currently surveying the possibility of including a test of this kind as a standardized type test for off-circuit tap changers, a product closely related to OLTCs. This test shows many good characteristics when it comes to mimic the product reality as it is experienced in the field. As was discussed above, there remains some problems primarily with a more robust definition of how to perform the test and with a theoretical background. The test presented here has aimed at contributing to this improvement process.

One such problem, which also was encountered during the experimental part of this thesis, is the formation of a temperature gradient in the oil tank. This gradient will, as follows from Arrhenius relationship, make the contacts at different heights of the tank age differently. A resolution of this problem is to implement more oil pumps, increasing the circulation of the oil in the tank. This was also done in the present implementation with quite small temperature gradients as a result. The important thing is that the difference between the highest and lowest temperature is the same, not the timescale at which these are reached. If the warming and cooling is turned off for a few minutes while the pumps keep working, this will be accomplished. But here an additional arbitrary parameter is introduced, the oil circulation. In a type test, it should probably be defined in some way how much circulation that is allowed since the effects on the test result is uncertain.

Another question regarding the realization of the test is the oil in which the test should be performed. A reasonable approach is that the "worst" oil for which a product is said to work with, regarding oxidation aspects, should be used during the test. In the present test realization this was avoided due to a concern that the contacts would oxidize too quickly and thus not be a good topic for a Master's thesis. The oxygen concentration, which was uncontrolled in the present realization, is another interesting topic. First of all, what are typical levels of the oxygen concentration in operating transformers? How does this differ for different kinds of transformer oil such as inhibited oils?

An assumption that was made earlier, in equation (10) of section 3.4.2, stated that the contact bulk temperature increase is 45.3 °C under load current. This assumption can be checked retrospectively by comparison with table 6. From the table one can see that the increments are 12, 18 and 25 °C for Ag/Ag, Cu/Ag and Cu/Brass, respectively, the first day and that these then increases to 13, 42 and 133 °C, respectively. From this one can first draw the conclusion that different materials give rise to highly diverse values of bulk temperature increment. This, in turn, leads to that the contacts experience different effective levels of aging. But a good OLTC design should in principle not be punished for being good, and be stressed harder in an oxidation endurance test. In our test it turns out that the contact material which is standard on these types of tap selector, namely Cu/Ag, records a value very close to the assumption made after 20 days of testing. It can also be thought that the other material combinations, in a tap selector which they are designed for, would record values closer to the 45 °C. The assumption can therefore be thought to be legitimate.

A test which takes 30 days is both cumbersome and expensive to perform. A proposal to decrease the testing period, theoretically to half the one of today, is to use both the automized test proposed here which can age the test object during the night, and to increase the oil temperature to 130 °C. With the double amount of hours of aging compared with the AAFL test and the double acceleration factor compared to what is used here (with an oil temperature of 120 °C) it follows from the Arrhenius relationship that the test can be performed in 15 days, which feels much more feasible. The result of a test designed that way, of course, needs to be verified.

We argue that this particular modification is safe and really should be implemented in future test designs. The higher oil temperature is already used in the AAFL test with good results, and to extend the aging time each day is only a minor change. Some thought needs to be put to the calibration of the thermal deformations, though, but this seems like a manageable task.

Another way to speed up the aging is to raise the load current further. Tests have been performed elsewhere with triple the rated current. Problems

can appear with contact solutions that do not cope with this higher level of load current, though, and it is thus doubtful if this is a good way to go. One should also be cautious not to shorten an accelerated life test too much by putting more stress on the test object, since new failure modes can appear and important failure modes in real life operation can be omitted. The even higher contact temperature could initiate chemical reactions that either hasten the failure of contacts, or postpone it. Ten degrees more could for example induce unforeseen reactions with the oil which would shorten the expected life of the contact, or it could "clean" the contacts by dissolution of oxygenized metal. Again, experimental testing and verification with expected results needs to be performed.

A very interesting topic is the one regarding the verification of the claim that the accelerated life test corresponds to 30 years of real life aging. The straight forward approach is to prepare a reference test which is left during said timespan, with which the accelerated tests can then be benchmarked. There are better, and probably faster, ways to accomplish verification to a satisfying degree, though. One verification proposal is to send out a voluntary questionnaire to grid operation companies. Questions of value to include are which models of tap changers they have used, how they have been used (are they prone to failure due to oxidation?), how have they performed and have some models lead to failure? If they are willing to collaborate and if a large enough response rate is reached, the outcome could be reassuring before a standardized type test is implemented.

Last but not least, we will take a look at our criteria. The general criteria are designed to be valid even as contacts develop, where both the constant $c_1$ and the allowed confidence interval can be modified. $c_1 = 3$ is derived by assuming that Cu/Ag, the present standard contact, should narrowly pass the test. With $c_1 = 3$, only 2 out of 5 Cu/Ag pass. We have not considered what percentage of passed contacts should be necessary for a material combination to be approved since our evaluation test only had five contacts. With more data, this can hopefully be determined, and should perhaps be incorporated in the test as an extra criterion. The fact that so many of the industry standard contacts failed does not discredit neither the contacts nor our tests, that is only because we set it to be hard on the present contacts, expecting future solutions to perform better. If Cu/Ag remains a dominant solution for much longer, and its performance is deemed satisfactory by costumers and norm committees, the value of $c_1$ should perhaps be even more generous.

The main advantage with our criteria is that the stability criterion is quantified in a simple way, leaving less room to the test performer to interpret results freely. The resistance rise criteria is actually the same as in the AAFL, except that we use the result of the third day as the reference to avoid

misleading results for materials with high initial resistance that goes down after only a short while. Of course, our allowed resistance raise is higher, but this is because we believe that the power cycles we use will age the contacts more effectively, thus causing a higher raise than the AAFL aging.

## 6.2  Silver Iodide and the Surface Structure of Silver Contacts

The SEM analysis showed several examples of pores on the fixed Ag(p) surfaces, which are electroplated silver on a bulk copper contact. These were of different sizes and shapes, often oval like, and could very well be the pores detected by Lowery in [27]. In that article, the smallest pores detected were $2.5\,\mu$m. We could detect much smaller pores than that, but we were not able to quantify their depth and density, an information which could be useful in determining the probability of AgI accumulating in them.

The SEM could not be used to detect AgI in the pores. We had hoped to run very local EDX analysis and see exactly where the AgI was located, but did not manage. Infact, the SEM did not contribute with much new information on AgI coated contacts all together. On the unworn surfaces the AgI cover was too thick to reveal any microstructures below it. In the worn tracks, we could not see any difference between AgI coated and regular Ag surfaces.

Our results supported the theory that AgI could be accumulated in pores and scratches on the surface, presented by [19], in the sense that we found pores and crevices on the silver surface, which were still present after 400 operations. Since the existence of pores is a prerequisite for the theory to be valid, this is in its favour. The theory can thus not be exclude since the possibility remains that AgI can accumulating in pores of the surface, as the theory proposes. A further prerequisite for the theory to explain the continued presence of AgI would be that the pores and crevices in the worn tracks were still present after hundreds of thousands of operations. This is something our experiment did not have the ambition to show, but which could be the topic of fruitful future study. It would also be valuable with a quantitative analysis of the size, depth and surface density of the pores to estimate how much AgI they could possibly hold. This could be a guiding fact in evaluating the probability of the proposed theory being correct.

# References

[1] L. Johnsson. Reliability and service characteristics on abb tap-changers and bushings. Ludvika, Sweden, January 2006. 1ZSC001535-AAA.

[2] On-load tap-changers, type uc and vuc. technical guide. `http://search.abb.com/library/ABBLibrary.asp?DocumentID=` `1ZSE5492-105&DocumentPartID=&Action=Launch`, Ludvika, Sweden, 2009. 1ZSC001535-AAA.

[3] P. G. Slade, editor. *Electrical Contacts : Principles and Applications.* CRC Press, Boca Raton, FL, USA, 1999.

[4] IEC. Tap-changers – part 1: Performance requirements and test methods. Technical report, International Electrotechnical Commission, Geneva, Switzerland, 2003. Reference number: IEC 60214-1:2003.

[5] Unapproved ieee draft standard general requirements for liquid-immersed distribution, power,and regulating transformers (revision of ieee c57.12.00-2000). *IEEE Std PC57.12.00/D2*, 2002.

[6] J. Erbrink, E. Gulski, J. Smit, and R. Leich. Experimental model for diagnosing on-load tap changer contact aging with dynamic resistance measurements. 2009.

[7] H. Schellhase, R. G. Pollock, A. S. Rao, E. C. Korolenko, and B. Ward. Load tap changers: Investigations of contacts, contact wear and contact coking. pages 259–272, 2002.

[8] Ragnar Holm. *Electrical Contacts - Theory and Applications.* Springer, fourth edition edition, 1967.

[9] Michael D. Bryant. Resistance buildup in electrical connectors due to fretting corrosion of rough surfaces. *IEEE transactions on components, packaging, and manufacturing technology.Part A*, 17(1):86–95, 1994. Cited By (since 1996): 17.

[10] Å Kassman and S. Jacobson. Surface damage, adhesion and contact resistance of silver plated copper contacts subjected to fretting motion. *Wear*, 165(2):227–230, 1993. Cited By (since 1996): 8.

[11] Junhui Li and Abhijit Dasgupta. Failure-mechanism models for creep and creep rupture. *IEEE Transactions on Reliability*, 42(3):339–353, 1993. Cited By (since 1996): 11.

[12] Ch Poulain, L. Boyer, Ph Sainsot, M. H. Maitournam, F. Houze, M. Leclercq, J. P. Guery, and J. P. Charpentier. Experimental and theoretical study of creep effects in electrical contacts. pages 147–153, 1995.

[13] Wayne Nelson. *Accelerated testing : statistical models, test plans, and data analysis*. Wiley, New York, [rev. ed.] edition, 2004.

[14] Y. Kawahara. Evaluation of high-temperature corrosion life using temperature gradient corrosion test with thermal cycle component in waste combustion environments. *Materials and Corrosion*, 57(1):60–72, 2006. Cited By (since 1996): 4.

[15] E. Takano and K. Mano. The failure mode and lifetime of static contacts. *Parts, Materials and Packaging, IEEE Transactions on*, 4(2):51 – 55, jun 1968.

[16] P.J. Hopkinson. Electrical contacts for off-circuit tap changers for oil immersed transformers. `http://www.transformerscommittee. org/subcommittees/power/DETC/Paper-ElectricalContacts-DETC_ Oct2005.pdf`, October 2005.

[17] L. Dix and P. J. Hopkinson. Tapchangers for de-energized operation in natural ester fluid, mineral oil and silicone. 2009.

[18] Denergized Tap Changers Working Group. The following text is proposed to be added following the last paragraph of the clause as 7.2.2.1 of iec60214-1. `http://www.transformerscommittee.org/ subcommittees/power/DETC/F02-DETC%20thermal%20Endurance% 20test.pdf`, October 2002.

[19] S. Arnell and G. Andersson. Silver iodide as a solid lubricant for power contacts. pages 239–244, 2001.

[20] Ray F. Egerton. *Physical Principles of Electron Microscopy*. Springer, 1st edition, 2005.

[21] Chi Ma. Instructions for use of zeiss 1550vp field emission sem with oxford eds and hkl ebsd. `http://www.gps.caltech.edu/facilities/ analytical/sem/LEOSEM_CIT_v3.pdf`, September 2009.

[22] Michael D.G. Steigerwald. New detection system for leo fe-sem. `http://www.zeiss.com/C1256E4600307C70/EmbedTitelIntern/new_ detection_system_for_leo_fe-sem/$File/new_detection_system_ for_leo_fe-sem.pdf`.

[23] B-O Stenestam. Comments on functional life test. `http://www.transformerscommittee.org/subcommittees/power/DETC/S10-Comments%20on%20Functional%20Life%20Test.pdf`, March 2010.

[24] Svenska Kraftnät. Consumption by hour 2009. `http://www.svk.se/Global/06_Energimarknaden/Xls/Statistik/N_FoT2009.xls/`, May 2010.

[25] M.K. Biswas A.B. Hapase M.G., Gharpurey. The oxidation of vacuum deposited films of copper. *Surface Science*, 9(1):87–99, 1968. cited By (since 1996) 8.

[26] ABB AB. On-load tap-changers, types ucg, vucg and ucl with motor-drive mechanisms, types bue and bul - installation and commissioning guide. `http://www05.abb.com/global/scot/scot252.nsf/veritydisplay/4af8b2cebcdbdf5ec1257593003403fc/$File/1ZSE%205492-116%20en%20Rev%2010.pdf`, May 2010.

[27] Chris H. Lowery. Determination of porosity in silver electroplated copper leadframes by electrographic printing. pages 202–205, 1987. cited By (since 1996) 0.

# A   List of Components Used in Oxidation Endurance Test

The following is a list of the components used in the oxidation endurance test. Refer to figure 10 in section 3.6.1 for a structured overview of how to combine the components to realize the test.

| Component | Supplier | Model |
|---|---|---|
| Oil level switch | Stig Wahlström | LS-1950E |
| Temperature level switch | Acandia | TSA220C with sensor TG8 |
| Emergency stop | ABB | MEPY1-1024 |
| Manual circuit breaker | ABB | S202 |
| Control computer | | Generic MS Windows laptop PC |
| Control chassi | National Instruments | cDAQ-9174 |
| Relay | National Instruments | NI 9481 |
| Security contactors | ABB | A9 |
| Warming contactor | ASEA (now ABB) | EG 160 |
| Heat exchanger | Material laboratory ABB Ludvika | 18 kW |
| Magnetic water valve | Esska-teknik | 2340V220V00 |
| Measurement DC source | Exova | Delta Elektronika SM 15-100 |
| Load AC source | Material laboratory ABB Ludvika | 1200 A |
| Cooling water loop | Rinkaby rör | 2828 |
| Differential voltage drop measurement | National Instruments | NI 9205 |
| Thermocouple measurement | National Instruments | NI 9211 |
| Measurement current shunt | Exova | 1.5 mΩ |
| Oil | Nynäs | Nytro 10XN |

# B   Resistance Over Time of Individual Contacts



(a) 01, Cu/Brass

(b) 02, Cu/Brass
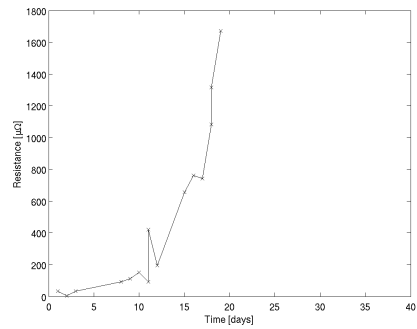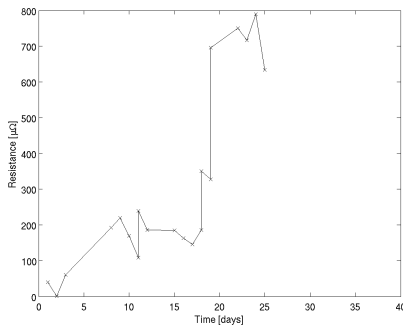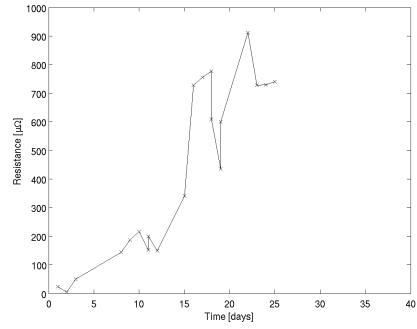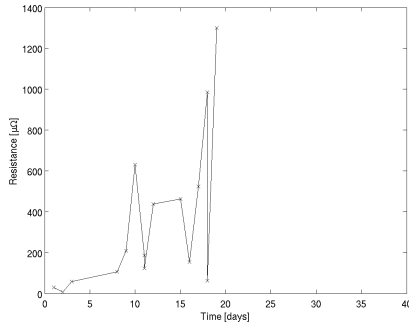
(c) 03, Cu/Brass

(d) 04, Cu/Brass
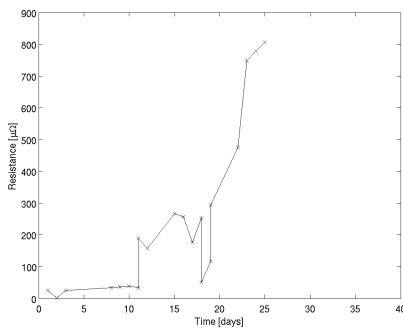
(e) 05, Cu/Brass

Figure 26: Resistance development over time of individual Cu/Brass contacts.
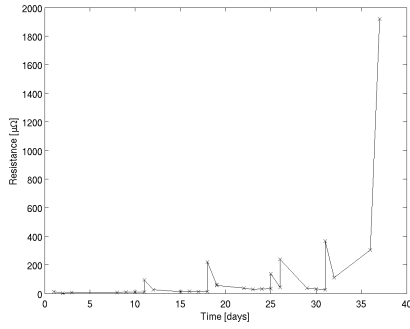
(a) 06, Cu/Ag
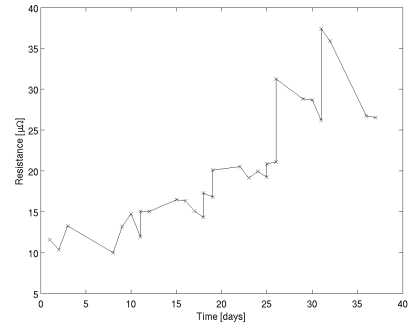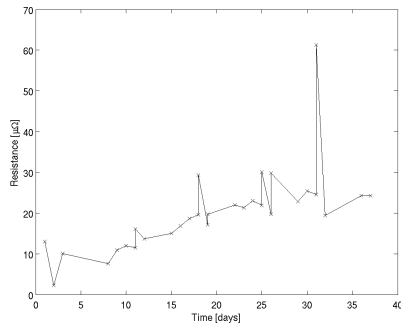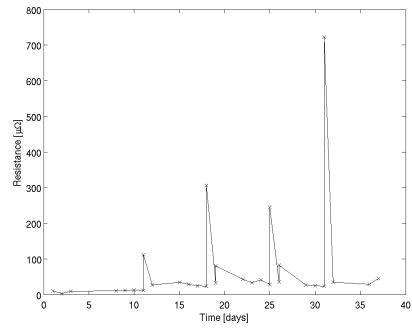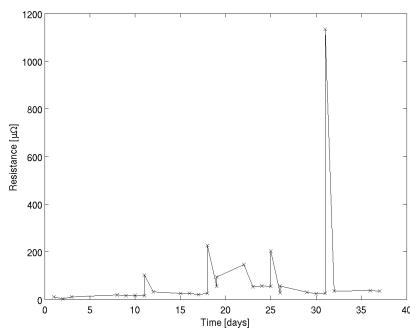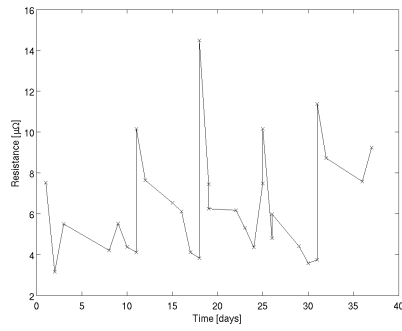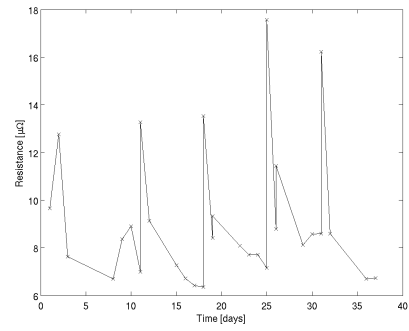

(b) 07, Cu/Ag


(c) 08, Cu/Ag


(d) 09, Cu/Ag


(e) 10, Cu/Ag

Figure 27: Resistance development over time of individual Cu/Ag contacts.

(a) 11, Ag/Ag
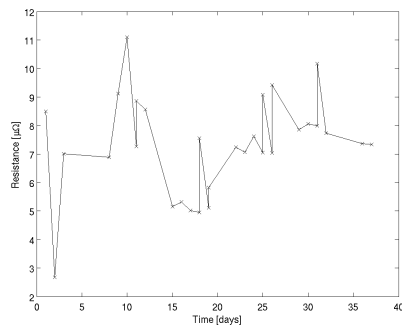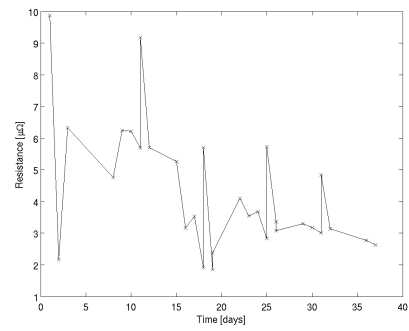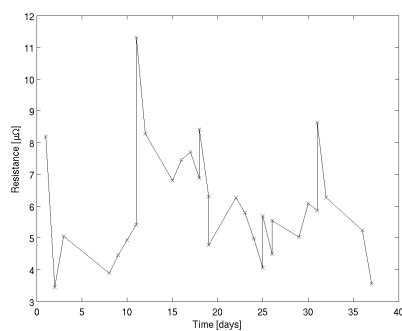
(b) 12, Ag/Ag

(c) 13, Ag/Ag

(d) 14, Ag/Ag

(e) 15, Ag/Ag

Figure 28: Resistance development over time of individual Ag/Ag contacts.

72